

The roles of vesicular GABA transporter
during embryonic development

Kenzi Saito

Doctor of Philosophy

Department of Biosystems Science

School of Advanced Sciences

The Graduate University for Advanced Studies

2010

CONTENTS

CONTENTS	i
ABBREVIATIONS	iv
ORIGINAL PUBLICATION	v
SUMMARY.....	vi
Background	1
1 Summary of inhibitory neurotransmission.....	1
2 VGAT.....	4
2.1 Molecular characteristics.....	4
2.2 Energy-dependence of VGAT.....	5
2.3 Expression of VGAT	7
3 Involvement of GABA in development of non-neural tissues	8
3.1 Morphogenic role of inhibitory neurotransmission.....	8
4 Non-vesicular release	10
4.1 Tonic inhibition.....	10
4.2 Control of the extracellular GABA level.....	11
4.3 Reverse transport of GAT-1	11
5 GABA in circuit formation	12
AIMS of the STUDY	14
MATERIALS AND METHODS.....	15
1 Animals	15
1.1 Construction of the Targeting Vector.....	15
1.2 Creation of a VGAT knockout allele.....	16
1.3 GAD67 knockout mice.....	16
2 Western blotting	17

3	Histology	17
4	Measurement of extracellular GABA concentrations and patch-clamp recordings in forebrain slice	18
5	Electrophysiological recordings in spinal cord	20
6	<i>In situ</i> hybridization of conditional VGAT knockout mouse.....	21
6.1	Tissue preparation	21
6.2	RNA probes	22
6.3	<i>In situ</i> hybridization	22
	RESULTS.....	24
1	Generation of conditional VGAT mice.....	24
2	Generation of VGAT ^{-/-} mice	29
3	Birth defects of VGAT ^{-/-} mice	31
3.1	Omphalocele and Cleft palate	31
3.2	Immobility and lower body weight in VGAT ^{-/-} fetuses	33
3.3	Reduction of trapezius muscle, hepatic congestion and decrease of alveolar spaces in VGAT ^{-/-} fetuses	35
3.4	Changes of neurotransmitter levels in forebrain	38
4	VGAT-independent GABA release in the forebrain.....	40
4.1	Lack of inhibitory synaptic transmission in VGAT KO striatal neurons.....	40
4.2	Presence of VGAT-independent GABA release in VGAT ^{-/-} forebrains.....	40
4.3	Tonic conductance in VGAT KO striatal neurons	41
5	Functional formation of VGAT KO spinal cord circuit.....	43
6	Comparison of developmental deficits between VGAT KO and GAD67 KO mice.....	49
	DISCUSSION	51
1	Increase in overall GABA and glycine contents in VGAT ^{-/-} forebrains.....	51
2	VGAT-independent GABA release	53

3	VGAT KO mice and motor circuit formation	54
4	Differences in phenotypic severity between GAD67 ^{-/-} and VGAT ^{-/-} mice	55
5	Developmental defects of non-neural tissues in mice with impaired inhibitory neurotransmission.....	56
	CONCLUSION.....	59
	ACKNOWLEDGEMENTS	60
	REFERENCES	61

ABBREVIATIONS

AMPA	α -amino-3-hydroxy-5-methyl-4-isoxazolepropionic acid
AP-5	D-2-amino-5-phosphonovaleric acid
CNQX	6-cyano-7-nitroquinoxaline-2,3-dione
CNS	central nervous system
Ctrl	control
DR	dorsal root
GABA	γ -aminobutyric acid
GABA _A R	GABA _A receptor
GABAT	GABA transaminase
GAD	glutamic acid decarboxylase
GAT	GABA transporter
GlyR	glycine receptor
IPSCs	inhibitory postsynaptic currents
KCC	K ⁺ -Cl ⁻ cotransporter
KO	knockout
MNs	motoneurons
NKCC	Na ⁺ -K ⁺ -2Cl ⁻ cotransporter
NMDA	N-methyl-D-aspartate
NSCLP	non-syndromic cleft lip with or without cleft palate
PCR	polymerase chain reaction
SNPs	single nucleotide polymorphisms
SVs	synaptic vesicles
VGAT	vesicular GABA transporter
VIAAT	vesicular inhibitory amino acid transporter
VMAT	vesicular monoamine transporter
VGluT	vesicular glutamate transporter
VACHT	vesicular acetylcholine transporter
VR	ventral root

ORIGINAL PUBLICATION

This thesis is based on the following original article and on some unpublished results. The article has been included at the end of the book.

Kenzi Saito, Toshikazu Kakizaki, Ryotaro Hayashi, Hiroshi Nishimaru, Tomonori Furukawa, Yoichi Nakazato, Shigeo Takamori, Satoe Ebihara, Masakazu Uematsu, Masayoshi Mishina, Jun-ichi Miyazaki, Minesuke Yokoyama, Shiro Konishi, Koichi Inoue, Atsuo Fukuda, Manabu Fukumoto, Kenji Nakamura, Kunihiro Obata, and Yuchio Yanagawa. The physiological roles of vesicular GABA transporter during embryonic development: a study using knockout mouse. *Molecular Brain* 2010 Dec 30; 3: 40

SUMMARY

This thesis describes the generation and analysis of vesicular GABA transporter (VGAT) KO mice to elucidate the functional role of VGAT during embryonic development. I have four main points of discussion: (1) generation of VGAT KO mice, (2) morphological defects in the VGAT KO mice, (3) VGAT-independent GABA release, and (4) spinal circuit formation in the absence of VGAT.

In the mammalian central nervous system, inhibitory neurons release GABA and glycine as neurotransmitters. In GABAergic neurons, GABA is synthesized from glutamate by two glutamic acid decarboxylases (GADs), GAD65 and GAD67. GABA is transported into synaptic vesicles (SVs) by a VGAT and is released from axon terminals by Ca^{2+} -dependent exocytosis. GABA activates either ionotropic GABA_A or metabotropic GABA_B receptors, which localize to either pre- or post-synaptic membranes. The activation of the receptors is terminated by the reuptake of GABA into axon terminals and/or glial cells by plasma membrane GABA transporters (GATs). As GABA and glycine share the same vesicular transporter and VGAT is thought to be the only vesicular transporter for inhibitory amino acids, VGAT is essential for inhibitory neurotransmission via SVs.

Recent gene KO studies on inhibitory neurotransmission have elucidated not only essential roles in neural functions but also an unexpected contribution to development of non-neural tissue. For example, deletion of the GAD67 gene leads to a non-neural developmental defect, cleft palate, and loss of VGAT results in cleft palate as well as omphalocele. Omphalocele is a herniation of the gut and liver through the umbilical ring. These studies have offered a conditional gene

KO technique for further understanding the role of inhibitory neurotransmission.

(1) Conditional VGAT mice based on the Cre/loxP system were generated. The conditional VGAT mice were crossed with mice expressing Cre recombinase in germ cells to obtain VGAT KO mice. Western blotting revealed the VGAT protein to be successfully eliminated from the VGAT KO brain. In addition, VGAT KO mice exhibited substantial increases in overall GABA and glycine, but not glutamate, levels in the forebrain, while the expression of GABA-synthesizing enzymes did not differ between controls and KOs.

(2) Although previous studies elucidated that the deletion of genes related to inhibitory neurotransmission leads to unexpected developmental defects such as cleft palate and omphalocele, rather less attention has been paid to other developmental abnormalities. To further explore the role of inhibitory neurotransmission in proper embryonic development, a comprehensive histological analysis was performed in controls and KOs.

VGAT KO mice were dead at birth, and had a cleft palate and omphalocele, confirming previously reported phenotypes. Their body weight at embryonic day (E) 18.5 was significantly lower than that of wild-type littermates. Histological examination revealed a decrease in trapezius muscle mass, hepatic congestion, and little alveolar space in the VGAT KO mice.

(3) In the last two decades, there is increasing evidence of neurotransmission outside synapses. Non-vesicular release is thought to be involved in this process. However, since it remains unclear to what extent the vesicular release contributes to the amount of GABA released, it is important to determine whether GABA is present in the extracellular space in the VGAT KO brain. To this end, whether or not GABA release could be confirmed in VGAT KO brain was investigated.

At first, GABA_AR-mediated synaptic currents were recorded using a whole-cell patch-clamp method. Electrophysiological recordings from E17.5 striatal neurons showed that the VGAT KO mice exhibited no spontaneous miniature inhibitory postsynaptic currents (IPSCs), suggesting the absence of vesicular release in the striatum. To investigate the presence of non-vesicular GABA release and the reversal of GAT-1, the amounts of GABA released from the forebrain slices were quantified. The slices were incubated in a small chamber containing artificial cerebrospinal fluid (ACSF) with or without a GAT-1 inhibitor, nipecotic acid, and the amount of GABA released into the ACSF was measured by HPLC. Without nipecotic acid, the amount of GABA in ACSF did not differ between controls and KOs. Blocking GAT-1 by nipecotic acid increased the amount of GABA in the ACSF. These results indicate that GABA can be released by VGAT-independent non-vesicular mechanisms in the embryonic mouse forebrain and that the plasma membrane GAT does not release, but rather than recovers the extracellular GABA.

(4) There is increasing evidence that GABA and glycine have neurotrophic effects in the developing nervous system, in which synapse formation are still immature. In such a situation, inhibitory neurotransmission must act non-synaptically. However, it is debatable whether or not vesicular GABA release is required for the neural circuit formation. To explore this issue, the responses to dorsal-root stimulation were examined in the control and VGAT KO mice.

Spontaneous IPSCs were absent in spinal cord motoneurons of VGAT KO mice. However, electrical stimulation of the dorsal root evoked excitatory, but not inhibitory, responses in the motoneurons. The latency of this excitatory response was similar to that of the control preparations. These results indicate that the sensory pathway to motoneurons is formed in the absence of GABA⁻ and

glycine-mediated synaptic responses. VGAT KO mice at E17.5-18.5 were completely immobile and stiff, and none of them responded to mechanical stimuli by pinching of the tail. Therefore, the lack of inhibitory transmission to motoneurons in VGAT KO mice likely resulted in defects in the spontaneous and stimulus-induced movements *in vivo*.

This study provides evidence that VGAT has an essential role not only in GABA- and/or glycine-mediated neurotransmission but also in embryonic development. Another significant achievement of this study is the generation of conditional VGAT mice. This provides an opportunity to further understand roles of GABAergic neurotransmission. For example, distinct groups of inhibitory neurons contain different peptides and different calcium-binding proteins. Different classes of inhibitory neurons have precise patterns of axon targeting. These distinct subtypes of inhibitory neurons appear to contribute to specific functions in the brain. The conditional VGAT mouse provides a new tool to study the subtype-specific and circuit-specific role of inhibitory neurons in brain functions.

Background

1 Summary of inhibitory neurotransmission

Figure 1 provides an overview of GABAergic neurotransmission. In GABAergic neurons, GABA is synthesized from glutamate by two glutamic acid decarboxylases (GADs), GAD65 and GAD67. GABA is transported into synaptic vesicles by a vesicular GABA transporter (VGAT) and is released from axon terminals via Ca^{2+} -dependent exocytosis. GABA activates either ionotropic GABA_A or metabotropic GABA_B receptors, which are localized to either pre- or postsynaptic membranes. The activation of the receptors is terminated by the reuptake of GABA into axon terminals and/or glial cells by plasma membrane GABA transporters (GATs)

Whereas GABA is ubiquitous in the central nervous system, glycine is best known as an inhibitory neurotransmitter in the brainstem and spinal cord. As GABA and glycine share VGAT for vesicular transport (Wojcik et al., 2006), GABAergic or glycinergic phenotype is specified by the cytosolic availability of GABA or glycine. Indeed, GABA and glycine can be coreleased from the same vesicles (Jonas et al., 1998; Kotak et al., 1998). As virtually all GABA is synthesized by GAD65 and GAD67 in embryonic brain (Ji et al., 1999), it is certain that these specify the GABAergic phenotype. On the other hand, specifying the glycinergic phenotype appears to require vigorous cytosolic accumulation even though glycine is a structural unit that makes up proteins. The key component is GlyT2, a plasma membrane transporter for glycine in neurons (Supplisson and Roux, 2002). Glycinergic neurotransmission was not detected in GlyT2 KO mice (Gomez et al., 2003). In the development of the auditory system, inhibitory neurotransmission of medial nucleus of the

trapezoidal body (MNTB) to the lateral superior olive (LSO) changes from GABA-dominant to glycine-dominant. In this synapse, the corelease of GABA and glycine from the same vesicles was observed, and the developmental decrease in GABAergic components appeared to parallel a decrease in GAD65 and GAD67 expression (Nabekura et al., 2004).

The effects of GABA_A and glycine receptor activation largely depend on the intracellular Cl⁻ concentration. In mature neurons, Cl⁻ equilibrium potential is more negative than the resting membrane potential for a relatively low intracellular Cl⁻ concentration. Therefore, the activation of GABA_A and glycine receptors causes Cl⁻ influx, leading to membrane hyperpolarization. This low Cl⁻ concentration is mostly due to the activity of potassium-chloride cotransporter 2 (KCC2), which exports the Cl⁻ (Delpire, 2000).

In certain circumstances, however, the activation of GABA_A and glycine receptors induces membrane depolarization (Ehrlich et al., 1999; Gao and Ziskind-Conhaim, 1995; Owens et al., 1996; Singer et al., 1998; Stein and Nicoll, 2003; Wu et al., 1992). In immature neurons, the expression of KCC2 is low and instead the expression of Na⁺- and K⁺-coupled cotransporter 1 (NKCC1) is high. Since NKCC1 promotes the Cl⁻ accumulation, the Cl⁻ concentration is high enough for Cl⁻ efflux via GABA_AR activation, leading to membrane depolarization (Delpire, 2000).

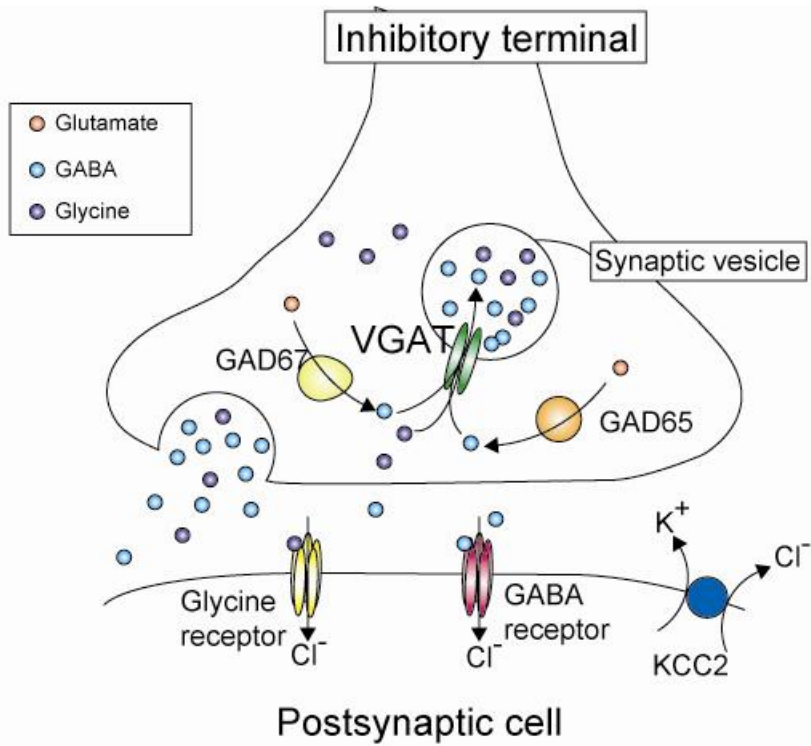


Figure 1. An overview of GABAergic neurotransmission.

2 VGAT

2.1 Molecular characteristics

The rodent VGAT cDNAs were identified by two separate groups based on genetic studies of *C. elegans*. *unc-47* of *C. elegans* had been predicted to function in the storage of GABA in presynaptic terminals (McIntire et al., 1993). In 1997, the same group predicted the amino acid sequence of the UNC-47 protein and identified its rat homologue. They further demonstrated that the rat *unc-47* homologue expressed in PC12 cells has a substantial ability to accumulate GABA. Finally, they concluded that the *unc-47* homologue is a vesicular GABA transporter (McIntire et al., 1997).

Sagné et al. independently identified a mouse VGAT cDNA based on a *C. elegans* genomic sequence covering *unc-47*. They also pointed out that VGAT mRNAs are localized to both GABAergic and glycinergic neurons in rat brain and VGAT-transfected cells significantly accumulated GABA and glycine. Conclusively, they denominate VGAT as VIAAT, short for “vesicular inhibitory amino acid transporter” (Sagné et al., 1997).

According to Ebihara et al. (2003), the mouse VGAT gene is extremely compact, spanning about 4.7 kb. The gene consists of three exons interrupted by two introns. They also proposed that there is an alternative splicing variant of VGAT. However, Oh et al. (2005) insisted that VGAT is composed of two exons and that the splicing variant is an artifact of PCR.

Exon 1 encodes a large, hydrophilic N-terminal domain and exon 2 and 3 encode a nine/ten-transmembrane domain and the C-terminal domain. Based on computer predictions, McIntire et al. (1997) suggested that VGAT has a cytosolic

localization for both N- and C-termini and a ten-transmembrane topology. Recently, using epitope-specific antibodies, Martens et al. (2008) proposed that the C-terminus faces the vesicle lumen and VGAT has a nine-transmembrane domain.

In this study, I planned to insert loxP sites into intron 1 and 3'-downstream of exon 2 and 3. As described above, since exon 2 and 3 encode a putative transmembrane domain, VGAT should be inactivated by Cre-dependent recombination of this region.

2.2 Energy-dependence of VGAT

Prior to the molecular cloning of vesicular transporters, the neurotransmitter uptake mechanism had been studied in purified SVs extracted from the brain. Driving force for neurotransmitter uptake into SVs is produced by a vacuolar H⁺-ATPase (V-ATPase), which raises a proton electrochemical gradient ($\Delta\mu\text{H}^+$). $\Delta\mu\text{H}^+$ is constituted of two components, the membrane potential ($\Delta\Psi$) and the pH gradient (ΔpH). Glutamate and monoamine (e.g. dopamine, serotonin, and noradrenalin) uptake predominantly depends on $\Delta\Psi$ (Bellocchio et al., 2000; Takamori et al., 2000a) and ΔpH (Varoqui and Erickson, 1996), respectively. GABA and glycine uptake, however, is driven by both $\Delta\Psi$ and ΔpH , because the accumulation partially inhibited when $\Delta\Psi$ is reduced or ΔpH is dissipated (Hell et al., 1991; Hell et al., 1990). Since GABA and glycine are neutral amino acids, the coupling of GABA uptake with a proton antiport (Hell et al., 1991) had been expected to be accompanied by the efflux of positive charge or influx of negative charge. Indeed, GABA and glycine uptake is Cl⁻-dependent (Hell et al., 1990; Kish et al., 1989). Recently, Juge et al. (2009) used reconstituted proteoliposomes containing VGAT to demonstrate that VGAT is a Cl⁻-GABA co-transporter. Figure

2 shows thermodynamics of VGAT.

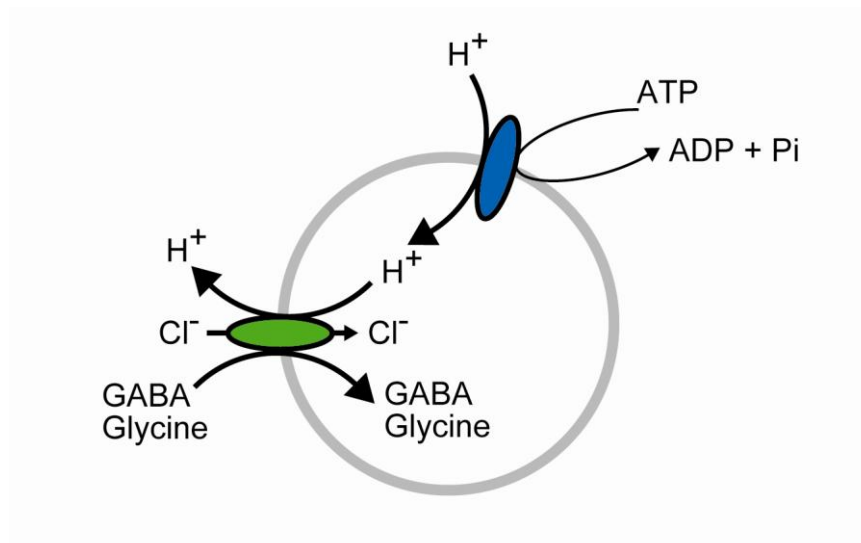


Figure 2. The stoichiometry of vesicular GABA/glycine transport.

The vesicular uptake of one neurotransmitter is coupled with one proton antiport. V-ATPase charges positively and acidified SVs, providing the driving force for neurotransmitter uptake. A Cl⁻ symport can provide an electrical shunt for efficient proton transport.

2.3 Expression of VGAT

After the molecular cloning of VGAT, development of an antibody specific to the VGAT elucidated its distribution. VGAT is localized to both GABAergic and glycinergic, but not glutamatergic, neuronal terminals (Chaudhry et al., 1998; Dumoulin et al., 1999; Takamori et al., 2000a).

The first evidence that VGAT/VIAAT is not expressed in non-neuronal tissues came from McIntire et al. (1997), who detected the 2.5-kb mRNA transcript in the brain, but not in twelve non-neuronal tissue samples (liver, kidney, lung, heart, gut, pancreas, spleen, ovary, testis, adrenal, muscle, and skin) by Northern blotting. However, they described that VGAT/VIAAT was detected in spleen, testis, and pancreas by RT-PCR. Later, several studies reported that VGAT/VIAAT was expressed in the pancreas (Chessler et al., 2002; Hayashi et al., 2003), pituitary (Mayerhofer et al., 2001), and testis (Geigerseder et al., 2003).

In the rat cerebral cortex, VGAT expression was low at birth, increased gradually through the first and second postnatal weeks and then achieved the adult pattern during the third postnatal week (Minelli et al., 2003). Using whole-mount *in situ* hybridization, Oh et al. (2005) reported that the VGAT mRNA is first detected at E10 in the ventral mesencephalon, hindbrain, and spinal cord and is widespread throughout the CNS at E11.5. These regions include the medial ganglionic eminence, a major source of cortical interneurons.

3 Involvement of GABA in development of non-neural tissues

3.1 Morphogenic role of inhibitory neurotransmission

GABA was first suggested to be a morphogen from studies on the teratogenic effect of diazepam over 30 years ago, where maternally-administered diazepam induced cleft palate in the offspring (Miller and Becker, 1975). Subsequent studies confirmed that GABA itself suppresses palatogenesis in utero and in culture (Tocco et al., 1987; Wee and Zimmerman, 1983; Zimmerman, 1985).

Further indications that GABAergic transmission has morphogenic roles come from studies with KO mice, in which genes related to inhibitory neurotransmission are deleted. However, there is a discrepancy between the old studies and recent genetic studies.

GAD67. Two independent studies found that the *GAD67* KO mice exhibited a cleft palate without other craniofacial malformations (Asada et al., 1997; Condie et al., 1997). Cleft palate is an anomaly with unfused palatal shelves. *GAD65* KO mice do not have such developmental defects (Asada et al., 1996; Kash et al., 1997).

GABRB3. The involvement of GABA in morphogenesis is further strengthened by cleft palate in mice lacking the GABA_AR $\beta 3$ subunit, *GABRB3* (Homanics et al., 1997). The $\beta 3$ subunit is widely distributed in the embryonic and adult brain (Fritschy et al., 1994; Laurie et al., 1992; Pirker et al., 2000). Although nineteen GABA_AR subunits have been cloned, there are no reports of similar developmental defects in KO mice lacking the other subunits (Boehm et al., 2004;

Vicini and Ortinski, 2004).

KCC2. Hubner et al. (2001) reported that *KCC2* KO mice display omphalocele, a herniation of abdominal organs through the umbilical ring. *KCC2* is required for GABA- and/or glycine-induced hyperpolarizing responses (Delpire, 2000). In the *KCC2* KO mice, GABAergic and/or glycinergic neurotransmission continued to act in an excitatory, but not an inhibitory, manner. In addition to having omphalocele, *KCC2* KO mice could not breathe properly and had lung atelectasis, a lack of gas in alveoli (Hübner et al., 2001).

VGAT/VIAAT. During the course of the present study, it was reported that *VGAT* KO mice display a cleft palate and omphalocele (Wojcik et al., 2006).

These studies not only provide new insight into the roles of inhibitory neurotransmission in non-neural tissue development, and they also shed light on the need for a conditional gene KO strategy to avoid the developmental influences frequently seen in conventional KO mice.

4 Non-vesicular release

4.1 Tonic inhibition

In research into inhibitory neurotransmission, considerable attention has focused on fast and precisely timed inhibitory neurotransmission, phasic inhibition. In phasic inhibition, postsynaptic GABA_ARs are activated by exposure to a high concentration of neurotransmitter via synaptic release (Owens and Kriegstein, 2002b). In the last two decades, there has been increasing interest in tonic inhibition, in which GABA_ARs primarily located outside synapses can be activated by a low concentration of extracellular neurotransmitter and are less desensitized (Farrant and Nusser, 2005). Tonic inhibition can be seen in cerebellar granule cells (Brickley et al., 1996; Chadderton et al., 2004; Hamann et al., 2002; Kaneda et al., 1995; Rossi et al., 2003; Wall and Usowicz, 1997), hippocampal CA1 interneurons (Semyanov et al., 2003) and pyramidal cells (Demarque et al., 2002; Glykys and Mody, 2007), dentate gyrus granule cells (Maguire et al., 2005; Stell and Mody, 2002), striatal GABAergic projection neurons (Ade et al., 2008), neocortical pyramidal neurons and interneurons (Olah et al., 2009), and olfactory bulb mitral cells (Wu et al., 2007). The nature of tonic inhibition varies with the area of the brain investigated and developmental stage.

While tonic currents are usually investigated in slice preparations or cultured neurons, their detection in cerebellar granule cells *in vivo* proves that the phenomenon is not an artifact of *in vitro* preparations (Chadderton et al., 2004). Tonic currents are usually measured as the difference in currents between the absence and presence of GABA_AR blockers. The properties of the source that releases the GABA responsible for tonic inhibition can be examined using various

treatments. As vesicular GABA accumulation and the subsequent release require $\Delta\mu\text{H}^+$ across the vesicle membrane and Ca^{2+} influx, respectively (see section 2.2), the currents in the presence of a $\Delta\mu\text{H}^+$ dissipater or under Ca^{2+} -free conditions could essentially be considered non-vesicular GABA release.

4.2 Control of the extracellular GABA level

Tonic inhibition is influenced by the extracellular amount of GABA. The amount is regulated by a buffering system (Cherubini and Conti, 2001; Glykys and Mody, 2007). Once released, GABA diffuses throughout synaptic cleft until it is taken up by plasma membrane transporters. High-affinity transport systems in the neuronal and glial membranes terminate the activation of GABA_{A} Rs and keep the extracellular neurotransmitter concentration low.

4.3 Reverse transport of GAT-1

While VGAT is located in the vesicular membrane and acts on transmitter storage into SVs, GATs distribute to the cell membrane of neurons and astrocytes and take up transmitters from the extracellular space. The uptake of GABA takes place in parallel with the co-transport of two sodium ions and one chloride ion into the cell (Kanner, 2006; Lu and Hilgemann, 1999). As reviewed in section.1, GATs are the most effective component of the GABA buffering system. However, a high intracellular sodium concentration could theoretically lead to the reversal of GATs (Attwell et al., 1993), and the reverse transport by GATs may be an important source of extracellular GABA.

Wu et al. investigated non-vesicular GABAergic transmission in cultured hippocampal neurons. They found that GABAergic transmission was not inhibited by four different methods generally used to block vesicular release. This

non-vesicular transmission was intensively blocked by GAT-1 antagonists, thus suggesting that GAT-1 actively releases GABA (Wu et al., 2007). Demarque et al. found tonic GABA_AR activation in developing hippocampal CA1 pyramidal neurons, in which synaptic contacts has not formed. In contrast to Wu et al., they showed that the tonic currents were not sensitive to a GAT-1 inhibitor, through the cellular mechanism of this tonic inhibition could not be defined (Demarque et al., 2002). Findings that do not support the involvement of GAT reverse transport have come from the GAT1 KO mouse. In this mouse, tonic currents were enhanced, suggesting that GAT-1 operates to recover the extracellular GABA (Jensen et al., 2003). Many researchers have reported that the tonic currents are enhanced rather than suppressed by GAT-1 blockers (Demarque et al., 2002; Olah et al., 2009; Rossi et al., 2003; Semyanov et al., 2003; Wall and Usowicz, 1997). Although the significance of reverse transport by GAT-1 is still controversial, it is certain that GAT-1 influences tonic inhibition by controlling extracellular GABA levels.

5 GABA in circuit formation

It has been widely recognized that GABA and glycine have a trophic role in the developing CNS (Ben-Ari, 2002; Ganguly et al., 2001; Kandler et al., 2002; Owens and Kriegstein, 2002b; Tapia et al., 2001; Varju et al., 2001). During the brain development, transmitter-evoked electrical activity is functional despite the immature synapse formation. As mentioned, GABA evokes the membrane depolarization in immature neurons, which is sufficient to cause Ca²⁺ influx (Ben-Ari, 2002; Ganguly et al., 2001; Liu et al., 2006; Owens et al., 1996). The percentage of neurons exhibiting an increase in Ca²⁺ in response to GABA gradually declines during neuronal development (Ganguly et al., 2001; Liu et al.,

2006). Using cultured neurons from embryonic rats, Ganguly et al. (2001) showed that this developmental transition of GABAergic action from depolarizing to hyperpolarizing is indeed mediated by GABA itself. They also showed that the transition was delayed by the blocking of GABA_ARs and correlated with an increase in KCC2 expression. Liu et al. (2006) observed similar phenomena in cultured chick neurons. Furthermore, GABAergic and/or glycinergic signals are involved in neural circuit formation in the retina (Blankenship and Feller, 2010). In contrast, the blocking of GABAergic and glycinergic transmission in spinal cord explants from rat embryos had little effect on the differentiation of the membrane properties of motoneurons (Xie and Ziskind-Conhaim, 1995). Also, despite the negligible presence of GABA in the brain, GAD65 and GAD67 double KO mice appeared to have a normal brain histology: the formation of the cerebellar Purkinje cell layer, and the growth of axons and dendrites occurred normally (Ji et al., 1999).

AIMS of the STUDY

The aims of this thesis are to establish conditional VGAT KO mice and to investigate the physiological roles of VGAT during embryonic development. The following are the specific aims.

(1) Although previous studies elucidated that the KO mice of genes related to inhibitory neurotransmission can lead to cleft palate and omphalocele, rather less attention has been paid to other developmental defects. To further explore the role of inhibitory neurotransmission in embryonic development, a comprehensive histological analysis was performed with controls and KOs.

(2) Although there is no doubt that synaptic neurotransmission is a basic form of inhibitory communication, there is increasing evidence of non-vesicular GABA release and tonic inhibition. However, since it remains unclear to what extent vesicular release contributes to the overall amount of GABA released, it is important to determine whether GABA is present in the extracellular space in the VGAT KO brain. To this end, whether or not GABA is released in the VGAT KO brain was investigated.

(3) Although the outstanding research with cultured VGAT KO neurons by Wojcik et al. showed that VGAT has a dominant role in the storage of GABA and glycine into SVs, it is unclear whether functional neural circuits are formed without vesicular GABA and glycine release. The functional importance of VGAT to the circuit formation was examined using electrophysiological recordings from the spinal cord.

MATERIALS AND METHODS

1 Animals

All animal procedures were conducted in accordance with the guiding principles of the NIH under the review and approval of the Animal Care and Use Committee of the Animal Care and Experimentation Committee, Gunma University, Showa Campus (Maebashi, Japan). Every effort was made to minimize the number of animals used and their suffering.

1.1 Construction of the Targeting Vector

Genomic BAC clones containing the mouse VGAT (mVGAT) locus were purchased, and the regions covering the entire VGAT gene were subcloned (Ebihara et al., 2003). A genomic fragment spanning exons 1-3 of the mVGAT gene was used for the targeting vector (Figure 3; targeting vector). The HindIII (in the 5'-flanking region) - KpnI (in the 3'-flanking region) fragment (7.5 kb) was subcloned into pBluescript II KS(-), and the 5'-loxP site was introduced into the XbaI site (in intron 1). The 5'-loxP site was flanked by a KpnI site artificially introduced for Southern blot analysis. The 7.5-kb fragment was used as the 5' homologous region containing the 5'-flanking region, exons 1-3, and the 3'-flanking region. The frt-flanked phosphoglycerate kinase (PGK) promoter-driven neomycin-resistance gene (PGK-Neo) cassette for positive selection of ES clones and the 3'-loxP site were inserted into the KpnI site (in the 3'-flanking region). The KpnI-BstEII fragment in the 3'-flanking region (3.5 kb) was added as the 3' homologous region. An MC1-DT-ApA cassette for negative selection (Yanagawa et al., 1999) was ligated to the 3' end of the homologous region.

1.2 Creation of a VGAT knockout allele

The linearized targeting vector was introduced by electroporation into ES cells (CCE) of 129/SvEv mouse origin, and G418-resistant colonies were screened by Southern blot analysis using probes outside of the targeting vector. KpnI-digested genomic DNA prepared from ES cell colonies was hybridized with 5' probes. The correctly targeted ES clones were injected into C57BL/6 blastocysts to produce germline chimeras. The germline chimeras were mated with C57BL/6 mice to establish the VGAT^{floxneo/+} mouse line. VGAT^{floxneo/+} mice were crossed with CAG-Cre mice (Sakai and Miyazaki, 1997) to excise exons 2 and 3 (VGAT knockout allele), and VGAT^{+/-} mice were obtained. Then VGAT^{+/-} mice were intercrossed to generate VGAT^{-/-} mice. When timed matings of the VGAT^{+/-} mice were performed, the morning of the day the vaginal plug was detected was designated E0.5.

Genotypes of VGAT^{+/+}, VGAT^{+/-} and VGAT^{-/-} mice were determined by PCR using the following oligonucleotides: primer P1 (5'-AGTCTGATCCCGTGGCACTTCCAACCTC-3') corresponding to intron 1 of the VGAT gene and primers P2 (5'-TCAGAGGCTTCTTCCTAGGGCTGCTG-3') and P3 (5'-GACCTCCCCCATTGCATAGAATGGCAC-3') corresponding to the 3'-flanking region of the VGAT gene. The primer set of P2 and P3 amplified a 183-bp fragment specific for the wild-type allele, and the primer set of P1 and P3 yielded a 430-bp fragment specific for the KO allele.

1.3 GAD67 knockout mice

Homozygous GAD67-GFP (Δ neo) (GAD67^{GFP/GFP}) mice were used as GAD67 KO (GAD67^{-/-}) mice. The generation of the GAD67-GFP (Δ neo) mice and their genotyping by PCR were described previously (Kaneko et al., 2008;

Tamamaki et al., 2003). In the GAD67-GFP (Δ neo) mice, a cDNA encoding enhanced green fluorescent protein (EGFP) followed by an SV40 polyadenylation signal was targeted to the locus encoding GAD67 by homologous recombination, and the GAD67 gene was disrupted.

2 Western blotting

Homogenates prepared from E18.5 mouse brain were separated by 7.5% SDS-polyacrylamide gel electrophoresis, transferred to nitrocellulose membrane (Whatman, Maidstone, UK), and probed with antibodies specific for VGAT (1:1000) (Takamori et al., 2000b), GAD65/67 (1:1000) (Asada et al., 1996), synaptophysin (1:1000) (Synaptic Systems, Goettingen, Germany), and β -actin (1:10000) (Abcam, Cambridge, UK). After the membranes were washed with Tris-HCl buffered saline containing 0.05% (w/v) Tween 20, the bound antibodies were visualized with horseradish peroxidase-conjugated goat anti-mouse IgG or anti-rabbit IgG (Jackson ImmunoResearch Laboratories, West Grove, PA) using the ECL Western blotting detection system (GE Healthcare, London, UK). Protein levels were quantified using Light Capture and its software (ATTO, Tokyo, Japan). Expression levels were normalized to β -actin or synaptophysin levels, and the values are expressed as means \pm SE. Statistical significance was assessed using Student's *t*-test.

3 Histology

VGAT^{-/-}, VGAT^{+/-} and VGAT^{+/+} mice at E18.5 were investigated. Samples were fixed in 10% (vol/vol) formaldehyde, dehydrated with a graded series of ethanol solutions, and embedded in paraffin. Three-micrometer-thick sections were prepared, immersed in xylene to remove the paraffin, rehydrated, and

stained with hematoxylin-eosin. VGAT^{+/-} and VGAT^{+/+} mice were mixed together and are referred to as control mice.

4 Measurement of extracellular GABA concentrations and patch-clamp recordings in forebrain slice

Coronal slices were obtained from E17.5 mice. Pregnant mice were deeply anesthetized through inhalation of halothane, and the brain was rapidly removed from the embryo and placed in cold (4°C), oxygenated, modified artificial cerebrospinal fluid (ACSF). The solution contained 220 mM sucrose, 2.5 mM KCl, 1.25 mM NaH₂PO₄, 12.0 mM MgSO₄, 0.5 mM CaCl₂·2H₂O, 26.0 mM NaHCO₃, and 30.0 mM glucose (330-340 mOsm). Coronal slices (400 μm) were cut in modified ACSF using a vibratome (VT-1000; Leica, Wetzlar, Germany). The slices were kept in oxygenated standard ACSF consisting of 126 mM NaCl, 2.5 mM KCl, 1.25 mM NaH₂PO₄, 2.0 mM MgSO₄, 2.0 mM CaCl₂, 26.0 mM NaHCO₃ and 20.0 mM glucose with 95% O₂-5% CO₂ at room temperature.

Whole cell patch-clamp recordings were performed as previously described (Yamada et al., 2007). The slices were transferred to a recording chamber on the stage of a microscope (BX51; Olympus, Tokyo, Japan) and continuously perfused with oxygenated, standard ACSF at a flow rate of 2 ml/min and 32°C. Striatal neurons in the slices were viewed on a monitor via a 40x water-immersion objective lens with an infrared differential interference contrast (IR-DIC) filter and a CCD-camera (ORCA-ER C4742-95; Hamamatsu Photonics, Hamamatsu, Japan).

Patch electrodes were fabricated from borosilicate capillary tubing 1.5 mm in diameter (GD-1.5, Narishige, Tokyo, Japan) using a pipette puller (P-97; Sutter Instrument, Novato, CA). The electrode resistance ranged from 6 to 8 MΩ.

The pipette solution contained 130 mM CsCl₂, 2 mM MgCl₂, 0.5 mM EGTA, 10 mM HEPES, 3 mM MgATP, and 0.4 mM GTP (pH 7.3 with CsOH). Membrane currents and membrane potentials were recorded using an Axopatch 700A amplifier and digitized at 2 kHz by a Digidata 1332A data-acquisition system (Axon Instruments, Union City, CA). Data were acquired using pClamp9 (Axon Instruments) software and stored on a hard disk for off-line analysis using Clampfit9 (Axon Instruments). Series resistance compensation was not applied. Whole cell recordings were performed in the voltage-clamp mode ($V_h = -60$ mV) in the presence of the AMPA/kainate receptor antagonist 6-cyano-7-nitroquinoxaline-2,3-dione, (CNQX; Tocris, Ellisville, MO) (10 μ M), the NMDA receptor antagonist D-2-amino-5-phosphonovaleric acid (AP-5; Tocris) (50 μ M), the GABA_B receptor antagonist CGP55845 (Tocris) (3 μ M), and tetrodotoxin (TTX; Wako, Osaka, Japan) (0.3 μ M). All drugs were applied by superfusion or pressure application from a micropipette in the vicinity of the recorded neurons. Values of amplitudes and interevent intervals in mIPSCs are expressed as means \pm SD.

Extracellular GABA and taurine concentrations were measured by HPLC. Slices were kept for 1 hour in oxygenated ACSF for recovery. Two coronal slices were then transferred to a submerged-type small chamber (1.5 ml volume) filled with filtered ACSF (Minisart; Sartorius, Göttingen, Germany) and aerated with 95% O₂-5% CO₂. The slices were incubated for 1h at 37°C in ACSF with or without nipecotic acid (300 μ M), and 120 μ l of supernatant was collected and stored at -80 °C for HPLC.

GABA and taurine concentrations were measured by HPLC with an electrochemical detection system (ECD-300 series; Eicom, Kyoto, Japan) as previously reported (Hashiguti et al., 1993; Nakahara et al., 2003). Each sample

was injected by an autoinjector (M231XL; Gilson, Lewis Center, OH) with a 20- μ l sample loop. A 5- μ m ODS column (150 x 3 mm, Eicom) was used as the analytical column and kept at 30 °C in a column oven (ATC-300; Eicom). The mobile phase consisted of 60 mM $\text{NaH}_2\text{PO}_4 \cdot 2\text{H}_2\text{O}$, 9.6 mM $\text{Na}_2\text{HPO}_4 \cdot 12\text{H}_2\text{O}$, 0.015 mM $\text{EDTA} \cdot 2\text{Na}$, and 30% methanol at pH 6.0. The mobile phase was filtered through 0.45- μ m membrane filters and degassed with a degasser (DG-300, Eicom). A flow rate of 0.5 ml/min was maintained using an isocratic pump (EP-300, Eicom). Data were recorded on a data processor (EPC-300, Eicom), and sample concentrations were determined by comparing the peak areas with an external standard. Total GABA, glycine, and glutamate levels in the E18.5 mouse forebrain were measured as described previously (Fujii et al., 2007; Tamamaki et al., 2003).

The drugs used were SR95531 (Sigma, St. Louis, MO) and nipecotic acid (Sigma).

5 Electrophysiological recordings in spinal cord

Embryos (E17.5-18.5) of control ($\text{VGAT}^{+/+}$; n = 19, $\text{VGAT}^{+/-}$; n = 12) and $\text{VGAT}^{-/-}$ (n = 30) mice were decapitated and eviscerated, and the spinal cord was removed by ventral laminectomy. The isolated spinal cord was placed in a recording chamber perfused with oxygenated Ringer's solution (118.4 mM NaCl, 3 mM KCl, 2.52 mM CaCl_2 , 1.25 mM MgSO_4 , 25 mM NaHCO_3 , 1.18 mM KH_2PO_4 , and 11.1 mM D-glucose aerated with 5% CO_2 in O_2) at room temperature. Recordings from motoneurons (MNs) in the isolated spinal cord were performed as described previously (Nishimaru et al., 2005). Briefly, visually guided whole-cell tight-seal recording of MNs was performed with patch electrodes pulled from thick walled borosilicate glass to a final resistance of 5-8 M Ω . The electrode tips were filled with 138 mM K-gluconate, 10 mM HEPES, 1 mM CaCl_2 ,

5 mM ATP-Mg, and 0.3 mM GTP-Li. Intracellular signals were amplified with a Multiclamp 700B amplifier (Molecular Devices, Union City, CA), digitized at 5 kHz with the Digidata 1440A data acquisition system (Molecular Devices) and saved on a hard disk for off-line analysis. Electrical recordings and the stimulation of lumbar ventral roots (VRs) were performed using glass suction electrodes. MNs were identified visually as cells with large soma in the ventral horn and by observing the antidromic firing activated by the electrical stimulation of the adjacent VR. Extracellular signals of MNs through the VRs were amplified 10,000 times and bandwidth-filtered at 0.1-3000 Hz with an AC amplifier (World Precision Instruments Inc., Sarasota, FL). Dorsal roots (DRs) were electrically stimulated (a single pulse: 100 μ s duration, 50-500 μ A in intensity) at 10-sec intervals by a glass-suction electrode placed in close proximity to the DR ganglia. All drugs (CNQX, AP5, strychnine, picrotoxin and bicuculline; Sigma-Aldrich, St. Louis, MO) were dissolved in Ringer's solution and bath-applied to the preparation. Analysis was performed using pClamp 10 software (Molecular Devices). Summary statistics report the mean \pm SE unless otherwise specified.

6 *In situ* hybridization of conditional VGAT knockout mouse

6.1 Tissue preparation

The brain was quickly removed, embedded in OCT compound (Sakura finetek), and frozen in 2-methylbutane pre-cooled by liquid nitrogen. Blocks were stored at -80°C until use for cryosectioning. Ten or 20 μ m-cryosections were mounted on silane-coated slides, and air-dried. Slides were kept at -80°C until processing for *in situ* hybridization.

6.2 RNA probes

Specific primers for VGAT were designed based on the cDNA sequences of VGAT and GAD67, respectively. Digoxigenin (DIG) -labeled transcripts were synthesized using an RNA labeling kit (Roche) by *in vitro* transcription. The specificity of these probes was proven by sense strand hybridization.

6.3 *In situ* hybridization

After postfixation in 4% paraformaldehyde-PBS followed by three washes with PBS, sections were acetylated for 10 min in 0.25% acetic anhydride in 0.1 M triethanolamine-HCl. After three washes in PBS, the section were preincubated for 1 h at 72°C with hybridization buffer in a chamber humidified with 1 x saline sodium citrate (SSC)(150 mM NaCl and 15 mM sodium citrate), and 50% formamide. The sections were then hybridized for 12-24 h at 72°C with 1 ng/μl of DIG-labeled probe for VGAT or GAD67 in the hybridization buffer. The sections were next treated at 72°C with the following solutions: (1) for 15 min and 30 min with 1 × SSC, 50%(v/v) formamide; and (2) for 30 min with 0.1 × SSC. After two brief washes with Tris-buffered saline (TBS)(100 mM Tris-HCl[pH 7.5], 150 mM NaCl) and one 5-min wash with TNT buffer (100 mM Tris-HCl[pH 7.5], 150 mM NaCl, and 0.05% Tween 20), the sections were put in blocking solution containing 1% blocking reagent (Roche) in TNT buffer for 10 min, and then incubated with alkaline phosphatase-labeled anti-DIG antibody (Roche) in the blocking solution for 1-2 h at room temperature. Following two brief washes with TBS and one 5-min wash with TNT buffer, the sections were pre-equilibrated with AP buffer (100 mM Tris-HCl[pH 9.5], 150 mM NaCl, and 10 mM MgCl₂). The coloring reaction was carried out in AP buffer containing 225 μg/ml of nitroblue tetrazolium (NBT) and 525 μg/ml of 5-bromo-4-chloro-3-indolyl phosphate (BCIP)

at room temperature with shading. The reaction was terminated by rinsing the sections in distilled water. Following rapid dehydration through an ascending ethanol series and clearing in xylene, the slides were coverslipped with Mount Quick (Daido Sangyo).

RESULTS

1 Generation of conditional VGAT mice

The targeting strategy used for the generation of VGAT KO mice is shown in Figure 3. Exons 2 and 3 encode the putative transmembrane domain and C-terminus of the VGAT protein (Ebihara et al., 2003; Sagné et al., 1997), and accordingly, the deletion of these regions was expected to destroy the function of the protein. Selection markers have been shown to affect gene expression. To enable removal of the selection marker, a PGK-Neo cassette flanked by *frt* sites was inserted into the 3'-flanking region, which can be removed with Flp recombinase. The advantage of this strategy is that it can be done *in vivo*, after germline transmission of the target allele, and the excision does not disturb the loxP-flanked region. Correctly targeted ES cell clones were microinjected into blastocysts to generate chimeric mice. These mice were then crossed with C57BL/6 mice to generate heterozygous mice carrying one floxneo allele (VGAT^{floxneo/+} mice).

VGAT^{floxneo/floxneo} mice were born at the expected frequency, did not have a cleft palate or omphalocele, and were overtly indistinguishable from their wild-type littermates. Western blotting showed that the level of VGAT protein in VGAT^{floxneo/floxneo} brains was no different from that in wild-type brains. These results suggest that a loxP sequence and a *frt*-flanked PGK-neo gene inserted into intron 1 and the 3'-flanking region of the VGAT gene, respectively, do not affect the expression of the VGAT protein (Figure 4A, B). The absence of the PGK-Neo cassette also did not show any influence on the VGAT expression either (data not shown). However, it is unknown whether two kind of conditional VGAT alleles have the same level of efficiency of recombination or not.

To establish whether the VGAT^{floxneo} allele is useful for the conditional inactivation of the VGAT gene, VGAT^{floxneo/floxneo} mice were crossed with mice in which Cre recombinase is driven by the Gng7 promoter (Gng7Cre) to obtain VGAT^{floxneo/floxneo}; Gng7^{Cre/+} mice (referred to this as conditional KO mice). Gng7, the G protein γ 7-subunit, is most highly expressed in GABAergic projection neurons in the striatum (Wang et al., 2001; Watson et al., 1994). In Gng7Cre mice, the Cre recombinase gene is knocked in Gng7 locus. Cre recombinase activity was found predominantly in the caudate-putamen, nucleus accumbens, and olfactory tubercle (Kishioka et al., 2009).

Conditional KO mice survived postnatally and had no obvious developmental defects. The loss of VGAT expression was monitored by *in situ* hybridization using a DIG-labeled VGAT RNA antisense probe. In control striatum, VGAT gene expression gradually increased during the first postnatal week. No such expression pattern was observed in the KO striatum (Figure 5). Furthermore, conditional KO mice showed severe motor deficits including hindlimb claspings, postural instability, and abnormal locomotor activity, consistent with a pivotal role for GABAergic projection neurons in motor control (Bolam et al., 2000; DeLong, 1990; Grillner et al., 2005). These observations indicate that the conditional VGAT mice established in this study would be useful for investigating various aspects of VGAT function during development and adult neurotransmission. In addition to solving the problem of perinatal lethality, the conditional VGAT mice can now be crossed to a mouse that express Cre recombinase in a region- and cell type-specific manner, providing the opportunity for manipulation of specific neuronal circuits.

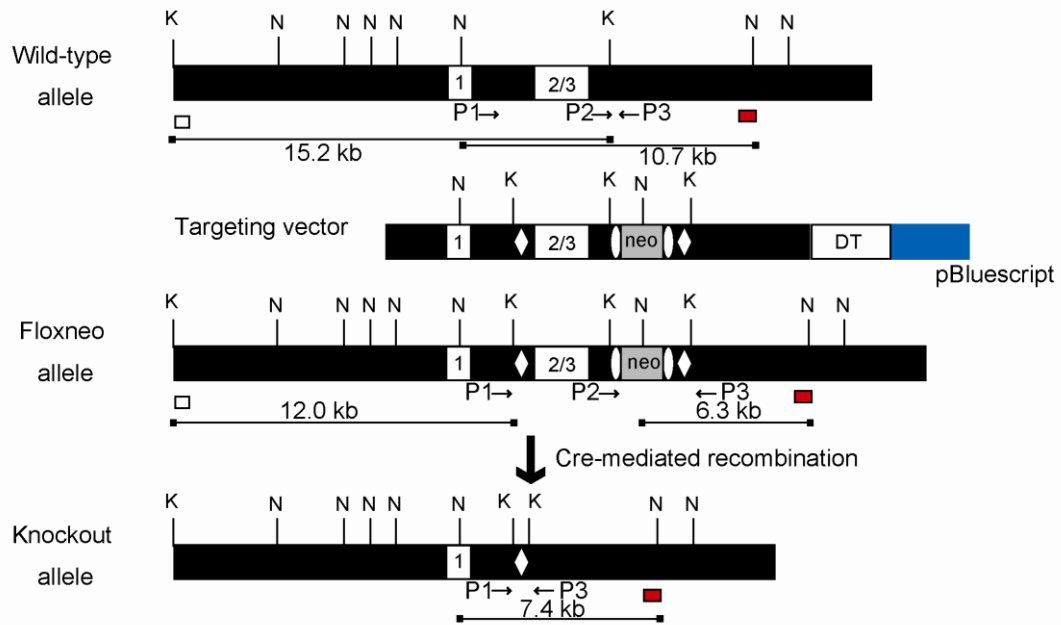


Figure 3. VGAT targeting strategy.

Exons are represented by numbered white boxes. *LoxP* sites (open diamonds) and a PGK-Neo cassette (*neo*; gray box) flanked by the *frt* sites (open ellipses) were introduced into the wild-type VGAT locus by homologous recombination to produce the floxneo allele. The probes used for Southern blot analysis are indicated as white (5' probe) and red (3' probe) boxes. The expected sizes of the *KpnI*- and *NcoI*-digested genomic DNA fragments hybridized with the 5' and 3' probes, respectively, are indicated as lines under the schemes. Relevant restriction sites are indicated as follows: K, *KpnI*; N, *NcoI*. PCR primers are indicated as arrows.

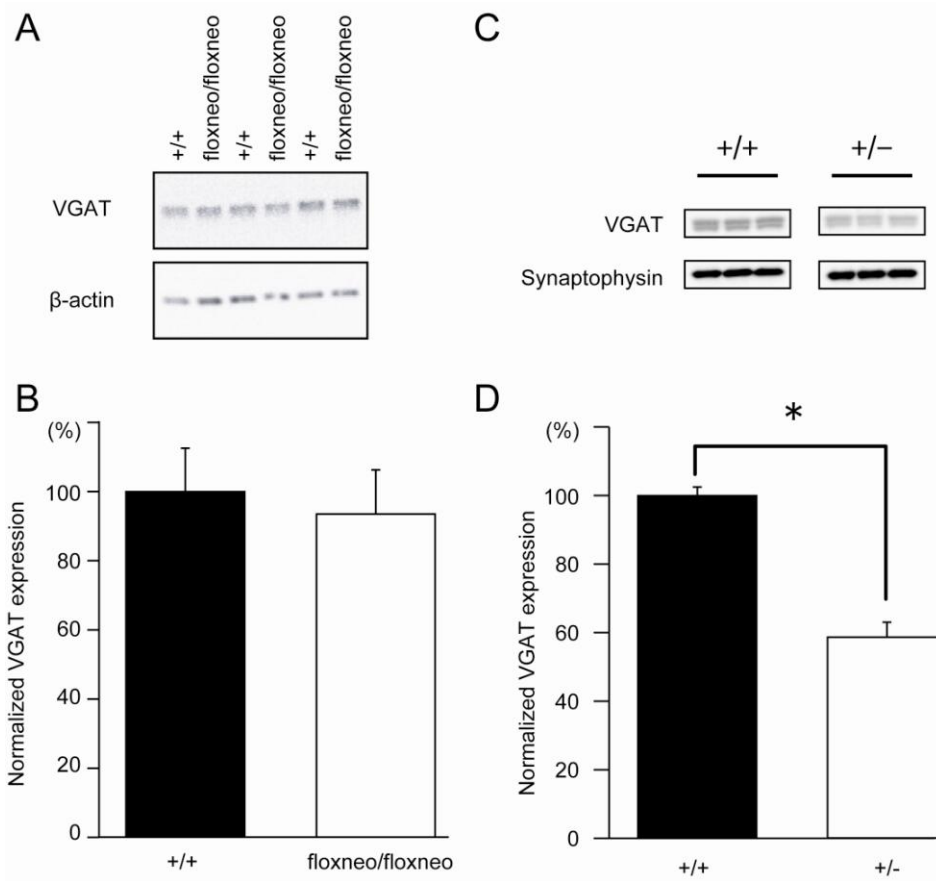


Figure 4. VGAT expression is normal in adult $\text{VGAT}^{\text{floxneo/floxneo}}$ and $\text{VGAT}^{+/-}$ mice.

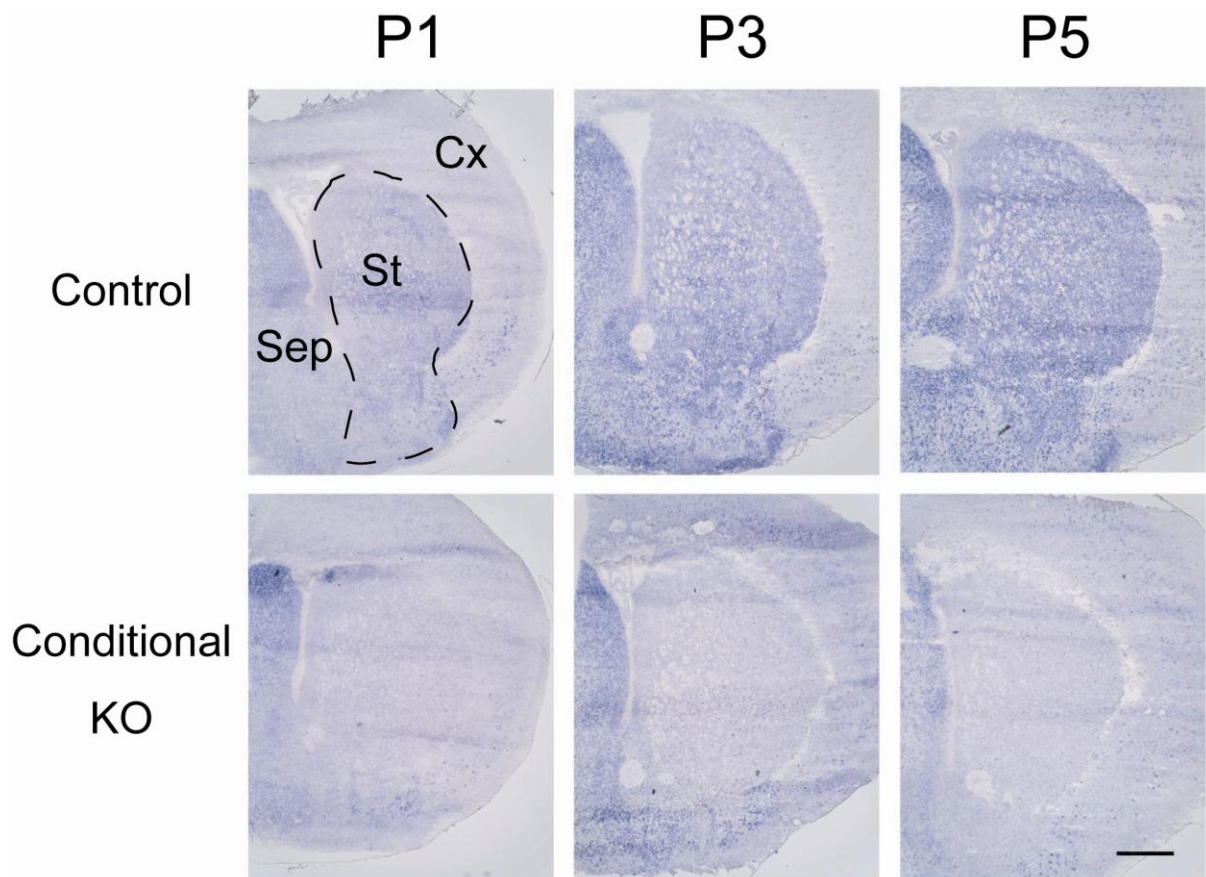


Figure 5. Striatum-specific deletion of VGAT.

Three control (upper panels) and three KO (lower panel) mouse brains were processed for *in situ* hybridization at postnatal day (P) 1, 3, and 5. Representative images are shown. VGAT mRNA expression gradually increased in the control striatum, while no such change was observed in the KO striatum. See the signal in septum as a reference for comparison. Abbreviations: St, striatum; Cx, cortex; Sep, septum. Scale bar = 500 μ m.

2 Generation of VGAT^{-/-} mice

The VGAT KO allele generated by crossing VGAT^{floxneo/+} mice with CAG-Cre mice, in which Cre recombinase is expressed ubiquitously (Sakai and Miyazaki, 1997). Genotyping was performed by Southern blot analysis (Figure 6A) and PCR (Figure 6B), and the DNA sequences around the loxP site in the KO allele were also confirmed (data not shown). VGAT^{+/-} mice were viable and developed normally to adulthood, except that their VGAT levels were reduced by about half (Figure 4C, D). To obtain homozygous VGAT KO (VGAT^{-/-}) mice, the VGAT^{+/-} mice were intercrossed. Western blot analysis revealed that no VGAT protein was expressed in the E18.5 VGAT^{-/-} brain, whereas VGAT expression in the VGAT^{+/-} mouse brain was reduced to about half of the WT level (Figure 6C).

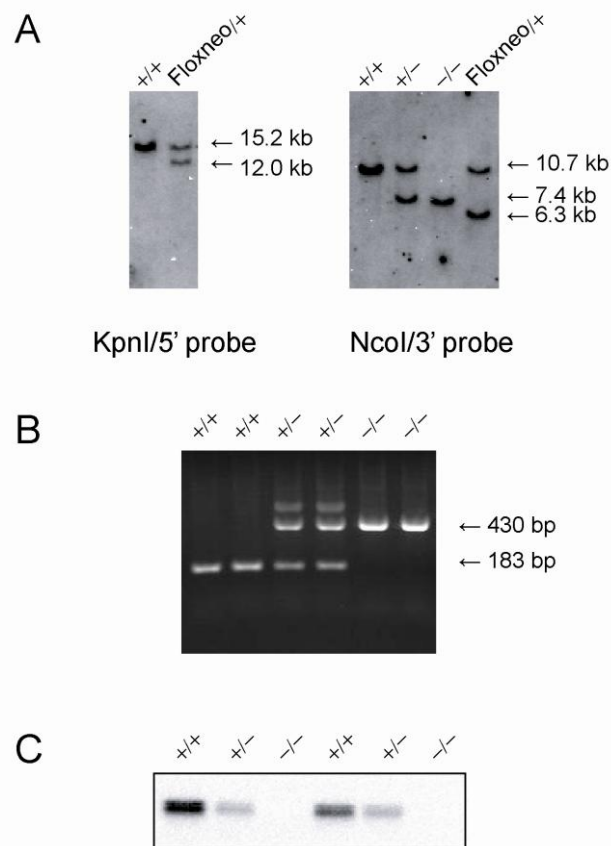


Figure 6. Disruption of the mouse VGAT gene

(A) Left, Southern blot analysis of KpnI-digested genomic DNA isolated from $VGAT^{+/+}$ ($+/+$) and $VGAT^{floxneo/+}$ (Floxneo/ $+$) mice using the 5' probe indicated in Figure 3. The wild-type allele corresponds to the 15.2-kb band, whereas the floxneo allele corresponds to the 12.0-kb band. Right, Southern blot analysis of NcoI-digested genomic DNA isolated from $VGAT^{+/+}$ ($+/+$), $VGAT^{+/-}$ ($+/-$), $VGAT^{-/-}$ ($-/-$), and $VGAT^{floxneo/+}$ (Floxneo/ $+$) mice using the 3' probe indicated in A. The wild-type allele, knockout allele, and floxneo allele correspond to the 10.7 kb, 7.4 kb, and 6.3 kb bands, respectively.

(B) Genotyping of offspring from intercrosses of $VGAT^{+/-}$ mice by PCR. Three primers were used (see Methods). Primers P2 and P3 produce a 183-bp fragment that represents the wild-type allele, whereas P1 and P3 produce a 430-bp fragment that represents the knockout allele.

(C) Western blot analysis of E18.5 whole brain homogenates from $VGAT^{+/+}$ ($+/+$), $VGAT^{+/-}$ ($+/-$), and $VGAT^{-/-}$ ($-/-$) mice using an anti-VGAT antibody directed against an N-terminal epitope. VGAT expression was completely abolished in $VGAT^{-/-}$ mice ($-/-$).

3 Birth defects of VGAT^{-/-} mice

3.1 Omphalocele and Cleft palate

All E18.5 VGAT^{-/-} fetuses displayed a cleft palate (Figure 7) and omphalocele (Figure 8), phenotypes consistent with those described by Wojcik et al. (2006).

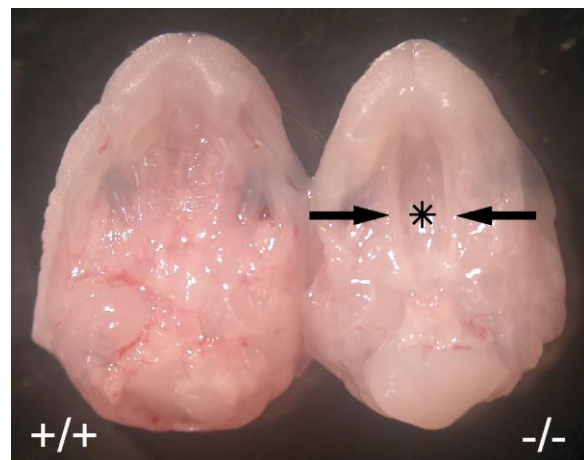


Figure 7. Cleft palate in VGAT^{-/-} mice

Ventral views of the upper jaw of E18.5 VGAT^{+/+} (+/+) and VGAT^{-/-} (-/-) mice. In contrast to the completely fused palate of VGAT^{+/+} mice, the secondary palatal shelves of VGAT^{-/-} mice do not contact each other (arrows), and the nasal cavity (asterisk) could be seen.

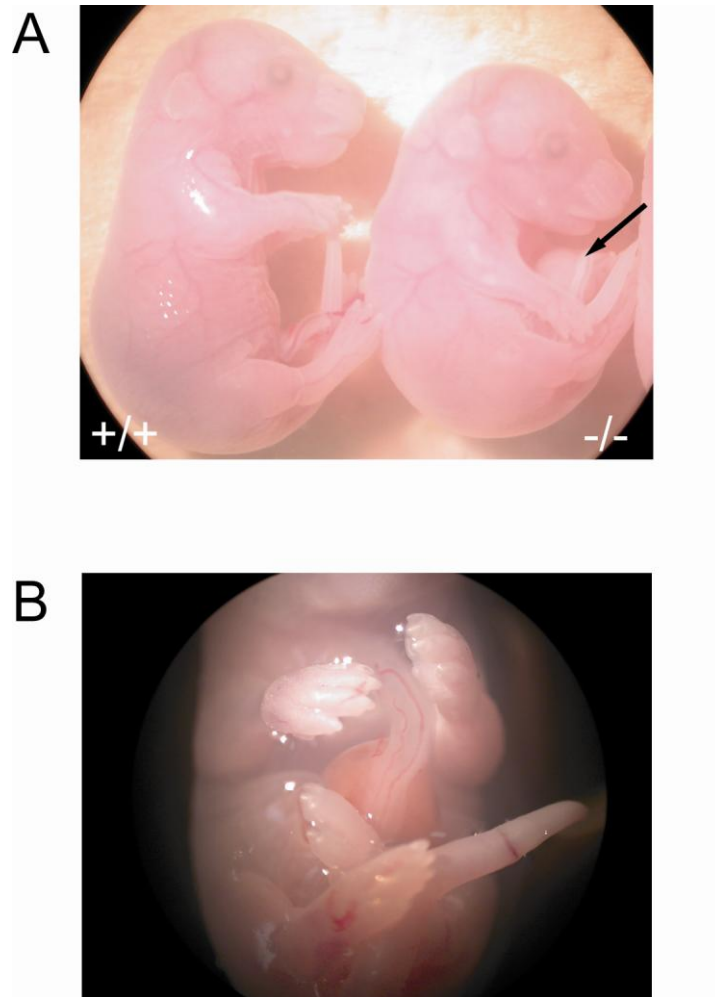


Figure 8. Omphalocele in VGAT^{-/-} mice

(A) Lateral views of E18.5 VGAT^{+/+} (+/+) and VGAT^{-/-} (-/-) mice. An arrow indicates omphalocele containing protruded organs in the VGAT^{-/-} mouse. In addition, the VGAT^{-/-} mouse showed an extremely hunched position in contrast to the VGAT^{+/+} mouse.

(B) Ventral view of the E18.5 VGAT^{-/-} mouse.

3.2 Immobility and lower body weight in VGAT^{-/-} fetuses

No VGAT^{-/-} mice survived beyond birth (Table 1). To estimate the time of death, we performed timed matings of the VGAT^{+/-} mice and obtained the fetuses via cesarean section. Among the E18.5 offspring derived from the intercrosses, VGAT^{-/-} fetuses were obtained at the expected Mendelian ratio (27.3%, 77 VGAT^{-/-} of 282 littermates) and more than 97% (75 of 77) were alive (as judged by umbilical beats or heartbeats, Table 1). When delivered by cesarean section on E18.5, both VGAT^{+/+} (7 of 7) and VGAT^{+/-} (11 of 12) fetuses began respiration, but none of the VGAT^{-/-} fetuses (n = 7) began to breathe, suggesting that VGAT^{-/-} mice died at birth due to respiratory failure.

The body weight of the E18.5 VGAT^{-/-} fetuses was significantly lower than that of VGAT^{+/+} and VGAT^{+/-} fetuses (VGAT^{+/+}: 1.18 ± 0.11 grams, n = 17; VGAT^{+/-}: 1.20 ± 0.08 grams, n = 45; VGAT^{-/-}: 1.05 ± 0.11 grams, n = 32 [mean \pm SD], P < 0.001, one-way ANOVA, post hoc Fisher's least significant difference test), indicating that VGAT^{-/-} mice exhibit growth retardation.

The hunched posture of the VGAT^{-/-} mice (Figure 8) suggests neuromotor dysfunction. To evaluate the neuromotor function of E18.5 fetuses, a tail pinching test was performed. VGAT^{+/+} (n = 16) and VGAT^{+/-} (n = 53) fetuses responded to the pinching with a twisting of the trunk. However, no such response was observed among the VGAT^{-/-} fetuses (n = 16), suggesting severely impaired neuromotor function.

Table 1. Genotypes of offspring from intercrosses of VGAT^{+/-} mice and phenotypes of VGAT^{-/-} mice

Age	Genotype			Phenotype		
	+/+	+/-	-/-	No. of -/- found dead	No. of -/- with omphalocele	No. of -/- with cleft palate
E18.5	69 (24.5%)	136 (48.2%)	77 (27.3%)	2/77 ^a	77/77 ^a	29/29 ^a
Newborn	22 (19.6%)	76 (67.9%)	14 (12.5%)	14/14 ^a	Not determined	Not determined

^a affected/examined

3.3 Reduction of trapezius muscle, hepatic congestion and decrease of alveolar spaces in VGAT^{-/-} fetuses

In previous studies on VGAT mutant mice, rather little attention has been paid to developmental defects other than cleft palate and omphalocele. To further explore the morphogenic function of VGAT, a comprehensive histological analysis was conducted.

Through the histological analysis of multiple tissues, marked changes were found in the trapezius muscle, ribs, liver, and lung. First, as can be seen in Figure 9A and B, trapezius muscle was thinner in VGAT^{-/-} fetuses than in the control fetuses. This result may be attributable to the stretching of the trapezius muscle due to the hunched posture of the fetus. However, it actually appears to be due to atrophy because the same phenotype was found when control and VGAT^{-/-} fetuses were sampled with care to keep similar posture. Second, the lower ribs were depressed, and their position was retracted toward the inside compared to the control (Figure 9C, D). Furthermore, the spaces between each rib appeared narrower in the VGAT^{-/-} mice (Figure 9C, D). Third, not only omphalocele (Figure 8) but also hepatic congestion was characteristic of VGAT^{-/-} embryos (Figure 9E, F). Together with the penetration of the abdominal cavity by the rib, it is obvious that VGAT^{-/-} liver is under external pressures. This indicates an increase in intra-abdominal pressure in VGAT^{-/-} fetuses. These results imply the hunched posture to be caused by an imbalance between the dorsal and ventral muscle strength, but it could not be ruled out that the thin trapezius muscle results from continuous stretching. Although omphalocele can be caused by a malformation of the ventral body wall (Brewer and Williams, 2004), the rectus abdominis muscle showed no apparent abnormality in VGAT^{-/-} mice (data not shown). Finally, the VGAT^{-/-} lung barely contained alveolar spaces compared to the control lung

(Figure 9G, H), indicating that the lungs had not been dilated. Consistent with the report by Fujii et al. (2007), who observed impairment of the respiratory network in VGAT KO mice, the VGAT^{-/-} mice lacked autonomous and joggling-induced breathing movements. A possible cause of atelectasis is reported to be a defect in the diaphragm (Baertschi et al., 2007). However, histological examination did not detect any difference in the diaphragm between the VGAT^{-/-} and control mice.

The alterations in the VGAT^{-/-} muscle, liver and lung were likely caused by the loss of VGAT in the CNS, but not the loss of VGAT in the peripheral tissue, because VGAT transcripts were detected in brain and spinal cord, but not in muscle, liver, or lung (McIntire et al., 1997; Sagné et al., 1997).

(Next page) Figure 9. Histological analysis of VGAT^{-/-} mice

(A, B) The trapezius muscle (bounded partly by white dashed lines) was thinner in VGAT^{-/-} mouse (B) than control mice (A). Scale bar: 200 μ m.

(C, D) The lower VGAT^{-/-} ribs (arrow in D) were depressed, and positioned on the inside compared to the control ribs (arrow in C). H, heart; L, liver.

(E, F) Red blood cell congestion was characteristic of VGAT^{-/-} liver, but not control liver. Scale bar: 200 μ m.

(G, H) The VGAT^{-/-} lung contained much less alveolar space than the control lung. Scale bar: 500 μ m.

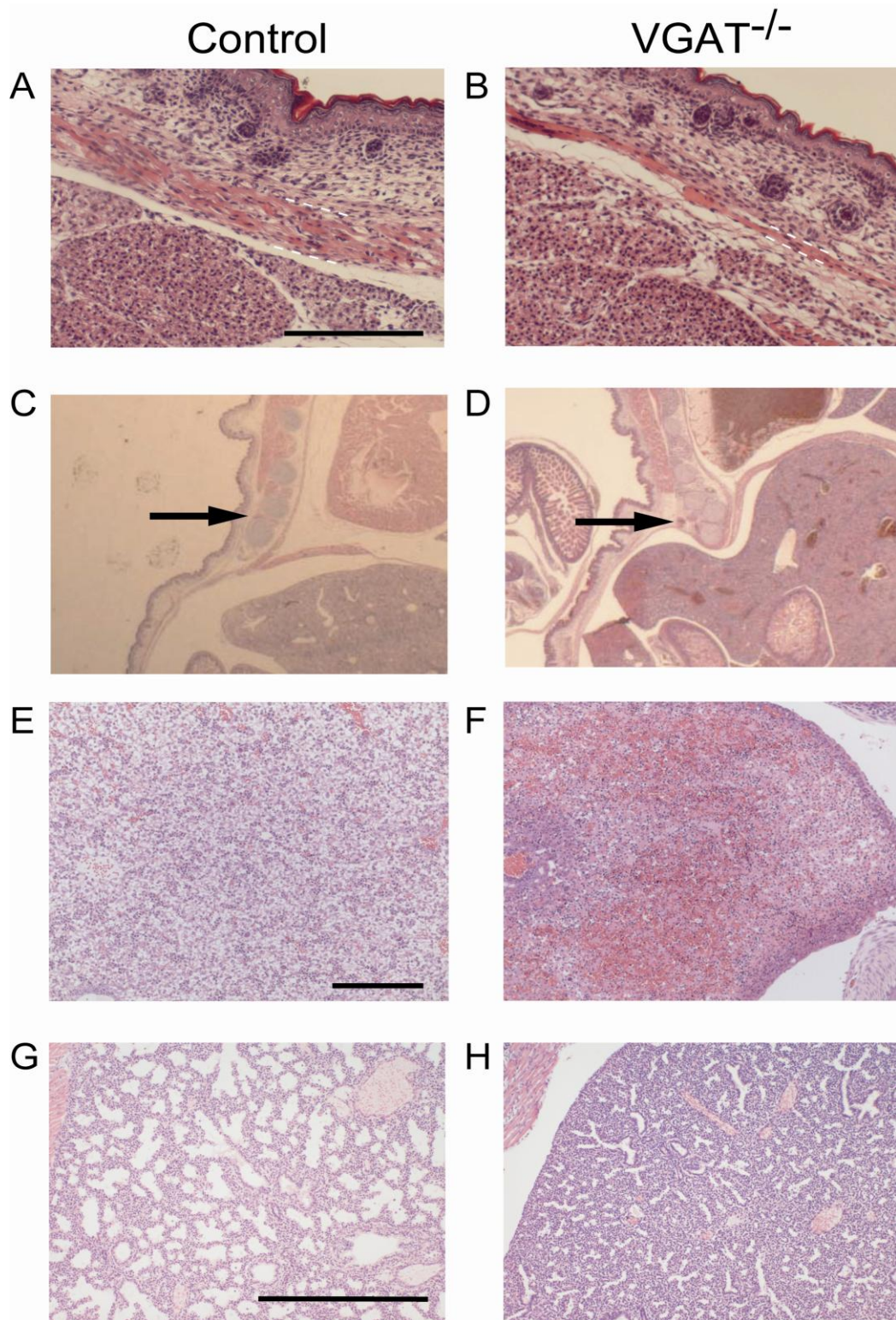


Figure 9

3.4 Changes of neurotransmitter levels in forebrain

As neurons are not capable of *de novo* synthesis of the neurotransmitters glutamate and GABA from glucose, they depend on glial cells for the supply of glutamine as the glutamate precursor (Bak et al., 2006). In addition, the system for degrading both GABA and glycine is mainly localized to glial cells (Cherubini and Conti, 2001; Sato et al., 1991). Thus, the metabolism of neurotransmitters is closely linked between neurons and glial cells. Given that loss of VGAT should impair the packing of GABA and glycine into SVs and the subsequent synaptic release, the neurotransmitter metabolism may be affected in VGAT^{-/-} mice.

To study whether the deletion of VGAT changes GABA/glycine levels, we measured the amount of the neurotransmitters GABA, glycine and glutamate in E18.5 VGAT^{-/-} forebrain by HPLC. As shown in Figure 10A, VGAT^{-/-} fetuses showed significant increases in GABA and glycine, but not glutamate, compared to VGAT^{+/+} fetuses. To test whether the increase in GABA was due to the elevated expression of GABA-synthesizing enzymes, I analyzed the expression of GAD65 and GAD67. A Western blot analysis showed that the expression levels of both GAD65 and GAD67 in VGAT^{+/+} and VGAT^{-/-} brains were similar (Figure 10B and C). These results indicate that the increase in GABA was not likely due to elevated levels of GABA-synthesizing enzymes in VGAT^{-/-} embryos.

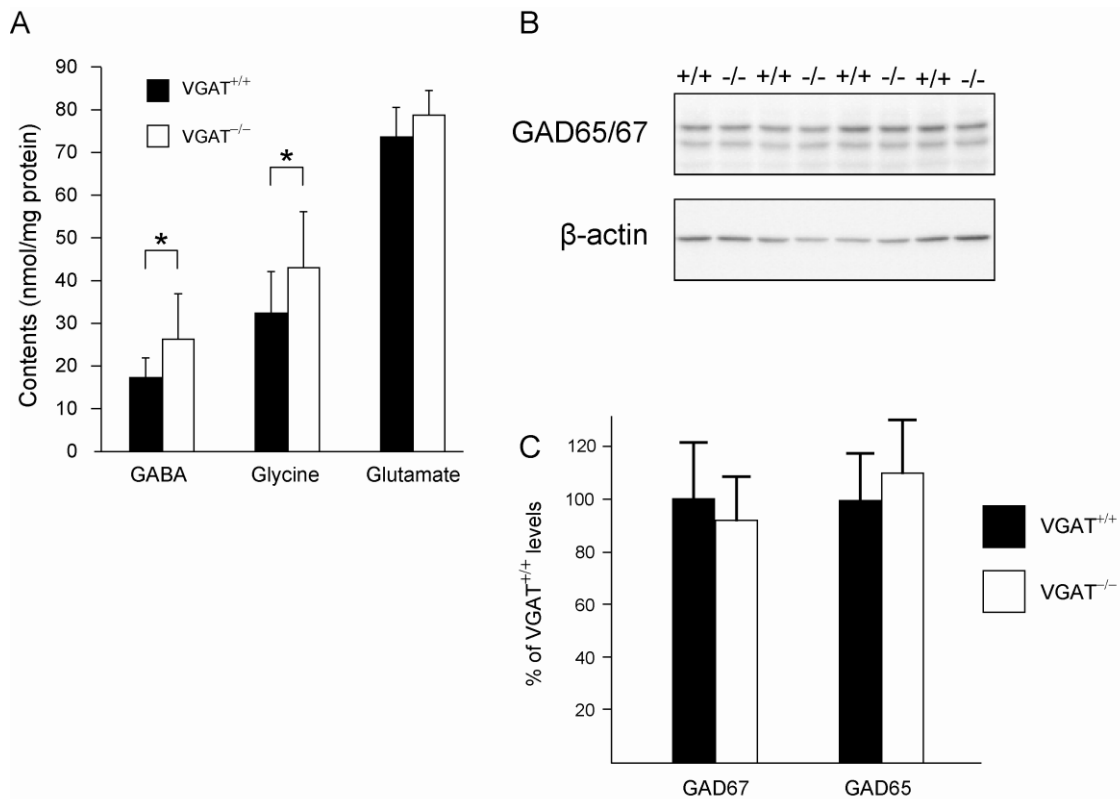


Figure 10. Neurotransmitter levels and the expression of GAD65 and GAD67.

(A) Neurotransmitter levels of E18.5 mouse forebrain. VGAT^{-/-} mice showed significantly higher levels of GABA and glycine, but not glutamate, than VGAT^{+/+} mice. Values represent means ± SD (*P<0.05; Student's *t*-test, n = 5-13 per group).

(B) Western blotting of GAD65/67, and β-actin. The expression levels of GAD65 and GAD67 in whole brain homogenate did not differ significantly between VGAT^{+/+} (+/+) and VGAT^{-/-} (-/-) mice. Equal amounts of protein were loaded and probed with an antibody that recognizes both GAD65 and GAD67.

(C) Quantification of GAD65 and GAD67 expression. Expression levels were normalized to β-actin expression. Data are presented as a percentage of VGAT^{+/+} levels. There were no significant differences (P = 0.80, Student's *t*-test).

4 VGAT-independent GABA release in the forebrain

4.1 Lack of inhibitory synaptic transmission in VGAT KO striatal neurons

To examine the effect of VGAT deficiency on GABAergic transmission in striatal neurons, we recorded GABA_AR-mediated synaptic currents using the whole-cell patch-clamp method. The pipette solution contained a high concentration of cesium chloride so that the GABA_AR-mediated currents at -60 mV were inward and most potassium currents were blocked (Yamada et al., 2007). GABA_AR-mediated mIPSCs were detected in VGAT^{+/+} mice (n = 2) and their amplitudes and interevent intervals were 22.9 ± 14.8 pA and 4.80 ± 6.74 sec, respectively (Figure 11Aa). In contrast, GABA_AR-mediated mIPSCs could not be detected in VGAT^{-/-} mice (n = 4) (Figure 11Ab). These results suggest that GABAergic synaptic transmission is absent in striatal neurons of VGAT^{-/-} mice.

4.2 Presence of VGAT-independent GABA release in VGAT^{-/-} forebrains

To investigate the presence of non-vesicular GABA release, we quantified the amount of GABA released from forebrain slices of E17.5 mice. The slices included cerebral cortex and striatum, and the striatum was composed predominantly of GABAergic neurons (Bolam et al., 2000).

As shown in Figure 11B, the extracellular GABA level at E17.5 was not significantly different from that in VGAT^{+/+} mice (Student's *t*-test, P = 0.91). It is worth noting that GABA can be released into the extracellular space in the absence of VGAT, as it could be detected in samples from VGAT^{-/-} mice.

Because non-vesicular GABA release can occur via a reversal of the plasma membrane GABA transporter GAT-1 under normal, non-pathological

conditions (Wu et al., 2007), it is possible that the extracellular GABA is derived from reverse transport by GAT-1. To determine the contribution of GAT-1 to extracellular GABA levels, similar experiments were conducted in the presence of a GAT inhibitor, nipecotic acid (Dalby, 2003). The addition of nipecotic acid increased rather than decreased the extracellular GABA levels in both VGAT^{+/+} and VGAT^{-/-} mice (Figure 11B, +Nipecotic acid), indicating that GAT-1 did not contribute to GABA release but actively removed GABA from the extracellular space.

4.3 Tonic conductance in VGAT KO striatal neurons

To clarify whether the extrasynaptic GABA contribute to the tonic response of striatal neurons in VGAT^{-/-} mice, a shift of GABA_AR-mediated tonic currents was examined by applying the GABA_AR antagonist SR95531 (10 μM). A high concentration of the drug blocks the phasic and tonic current, causing a change in the holding current (Brickley et al., 1996; Chadderton et al., 2004; Rossi et al., 2003). Bath application of SR95531 generated an outward shift of 3.1 ± 0.6 pA (n = 3; Figure 11C), corresponding to the suppression of a tonic inward current. This indicates that the extracellular GABA perpetually activates GABA_ARs of striatal neurons in VGAT^{-/-} mice.

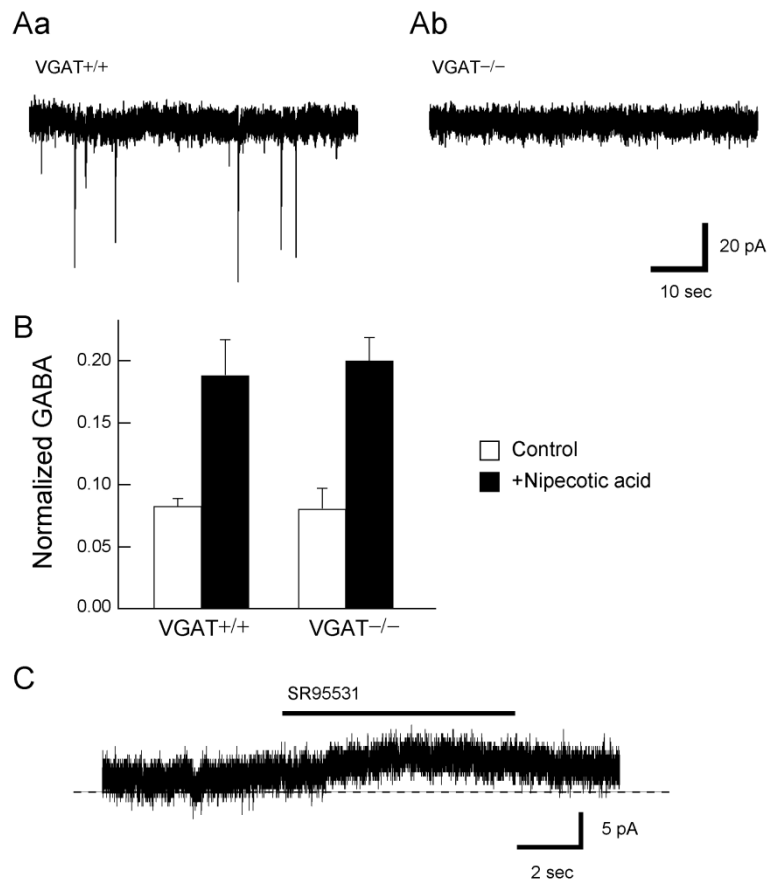


Figure 11. Extracellular GABA levels and GABA_AR-mediated currents in striatal neurons.

(A) Typical traces of spontaneous mIPSCs recorded from striatal neurons in VGAT^{+/+} (Aa) and VGAT^{-/-} mice (Ab). Spontaneous mIPSCs were detected in VGAT^{+/+} striatal neurons, but not in VGAT^{-/-} neurons.

(B) Extracellular GABA levels in coronal slices of VGAT^{+/+} and VGAT^{-/-} mice were measured by HPLC. The values shown were normalized to taurine content. The values of GABA for the VGAT^{+/+} (n = 7) and VGAT^{-/-} mice (n = 4) are shown (white bar). Extracellular GABA levels were comparable between VGAT^{+/+} and VGAT^{-/-} mice. Bath application of the GAT inhibitor nipecotinic acid further increased extracellular GABA levels in both VGAT^{+/+} (n = 4) and VGAT^{-/-} (n = 3) mice (black bar). Values represent means ± SE.

(C) SR95531 (10 μM) induced an outward shift of the holding current in a striatal neuron from a VGAT^{-/-} mouse. The dashed line depicts the holding current in the absence of SR95531.

5 Functional formation of VGAT KO spinal cord circuit

During the spinal reflex, synaptic inhibition plays a crucial role in coordinating the timing of the contraction of each muscle to generate movement (Peason and Gordon, 2000). Previous studies in rodents showed that the neuronal connections for this circuit are formed during the prenatal period and that functional inhibitory pathways are formed in embryonic spinal cords (Kudo and Yamada, 1987; Wu et al., 1992). GABAergic and/or glycinergic signals are involved in neural circuit formation in the retina (Blankenship and Feller, 2010). However, blocking GABAergic and glycinergic transmission in spinal cord explants from rat embryos had little effect on the differentiation of the membrane properties of motoneurons (Xie and Ziskind-Conhaim, 1995). It remains unclear how important GABAergic and/or glycinergic signals are to functional motorneuronal circuit formation. To explore this issue, dorsal-root-evoked motorneuronal responses (corresponding to the spinal reflex) were examined in VGAT KO mice.

First, to examine the physiological nature of synaptic inputs to spinal MNs, we performed whole-cell patch-clamp recordings using isolated spinal cord preparations taken from VGAT^{-/-} and control mouse embryos. In these preparations, the neuronal connections within the spinal cord remain relatively intact (Nishimaru et al., 2005). In control lumbar MNs, spontaneous outward currents were observed when the membrane was depolarized at -40 mV above the chloride ion reversal potential (approximately -78 mV in the present experimental condition). These currents were blocked by bath application of the glycinergic antagonist strychnine and the GABAergic antagonist picrotoxin, indicating that the currents were IPSCs (n = 8, Figure 12A). In contrast, no such spontaneous IPSCs were detected in VGAT^{-/-} MNs (n = 12, Figure 12B). When the

membrane potential was held at -70 mV, spontaneous inward currents were observed in both control and VGAT^{-/-} MNs (Figure 12). These inward currents were abolished by the concomitant bath application of the ionotropic glutamate receptor blockers CNQX (a non-NMDA receptor antagonist) and AP5 (an NMDA receptor antagonist), indicating that MNs received excitatory synaptic transmission in the VGAT^{-/-} spinal cord.

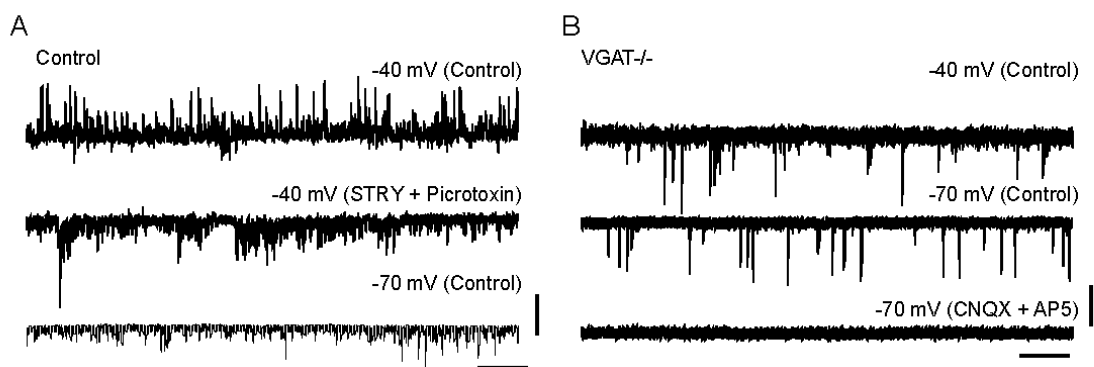


Figure 12. Representative whole-cell patch-clamp recordings from motoneurons (MNs) in a voltage clamp.

(A) In control motoneurons, spontaneous outward currents were observed when the membrane potential was held at -40 mV (upper trace). These currents were blocked by the bath application of strychnine (STRY, 0.5 μ M) and picrotoxin (50 μ M) (middle trace). Inward currents persisted in the presence of these antagonists and became prominent when the membrane potential was held at -70 mV.

(B) In VGAT^{-/-} MNs, no spontaneous outward currents were observed (upper trace). Inward currents observed at -70 mV (middle trace) were blocked by CNQX (10 μ M) and AP5 (50 μ M).

Vertical bars indicate 100 pA in A, 50 pA in B. Horizontal bars indicate 2 s (A, B)

Next, to test whether any functional motor circuits were formed in the VGAT^{-/-} spinal cord, electrical stimuli were delivered to DR and the motoneuronal responses were recorded, which correspond to the spinal reflex. During the spinal reflex, synaptic inhibition plays a crucial role in coordinating the timing of the contraction of each muscle to generate movement (Peason and Gordon, 2000). In rodents, the neuronal connections for this circuit are formed during the prenatal period, and functional inhibitory pathways are formed in embryonic spinal cords (Kudo and Yamada, 1987; Wu et al., 1992).

Electrical DR stimulation evoked compound action potentials in the lumbar VR both in control (n = 7) and in VGAT^{-/-} (n = 5) spinal cord. The latency of the response was similar in control (10.17 ± 0.31 ms) and VGAT^{-/-} (10.15 ± 0.24 ms) preparations, indicating that the functional connections from the periphery to MNs were present in the VGAT^{-/-} spinal cord. In control preparations, bath application of the inhibitory amino acid receptor blockers strychnine and bicuculline dramatically enhanced the DR-evoked response, revealing the strong inhibition underlying (Figure 13A). In contrast, the same set of antagonists had little effect on the VR response in the VGAT^{-/-} spinal cord (Figure 13B).

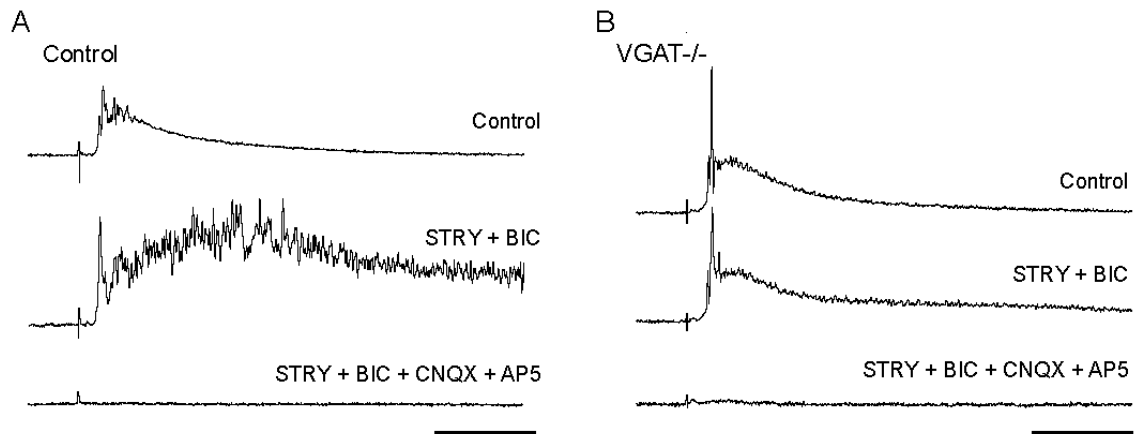


Figure 13. Dorsal root (DR)-evoked responses in the lumbar ventral root of the spinal cord.

(A) Strychnine and bicuculline (BIC, 5 μ M) significantly enhanced the area of the response ($728.9 \pm 148.7\%$ of the response before the bath application of the antagonists) (Student's t-test, $P < 0.01$).

(B) DR-evoked responses in the lumbar ventral root of the VGAT^{-/-} spinal cord. Strychnine and bicuculline did not significantly increase the response ($107.3 \pm 9.8\%$, $P > 0.5$). CNQX and AP5 blocked the evoked response in both control and VGAT^{-/-} spinal cord.

Vertical bars indicate 50 μ V. Horizontal bars indicate 50 ms.

Postsynaptic currents in MNs were evoked by the DR stimulation. In control MNs (n = 8), the outward currents were observed when the membrane potential was held at -40 to -50 mV. These outward currents were blocked by picrotoxin and strychnine, showing that they were indeed mediated by GABA and glycine (Figure 14A, C). The DR-evoked responses of VGAT^{-/-} MNs (n = 10) did not show any outward currents at these holding potentials (Figure 14B, D), indicating that there was little or no detectable inhibition involved in this pathway in spinal cord lacking VGAT. These electrophysiological data indicate that VGAT^{-/-} MNs do not receive functional synaptic inhibition mediated by GABA and glycine.

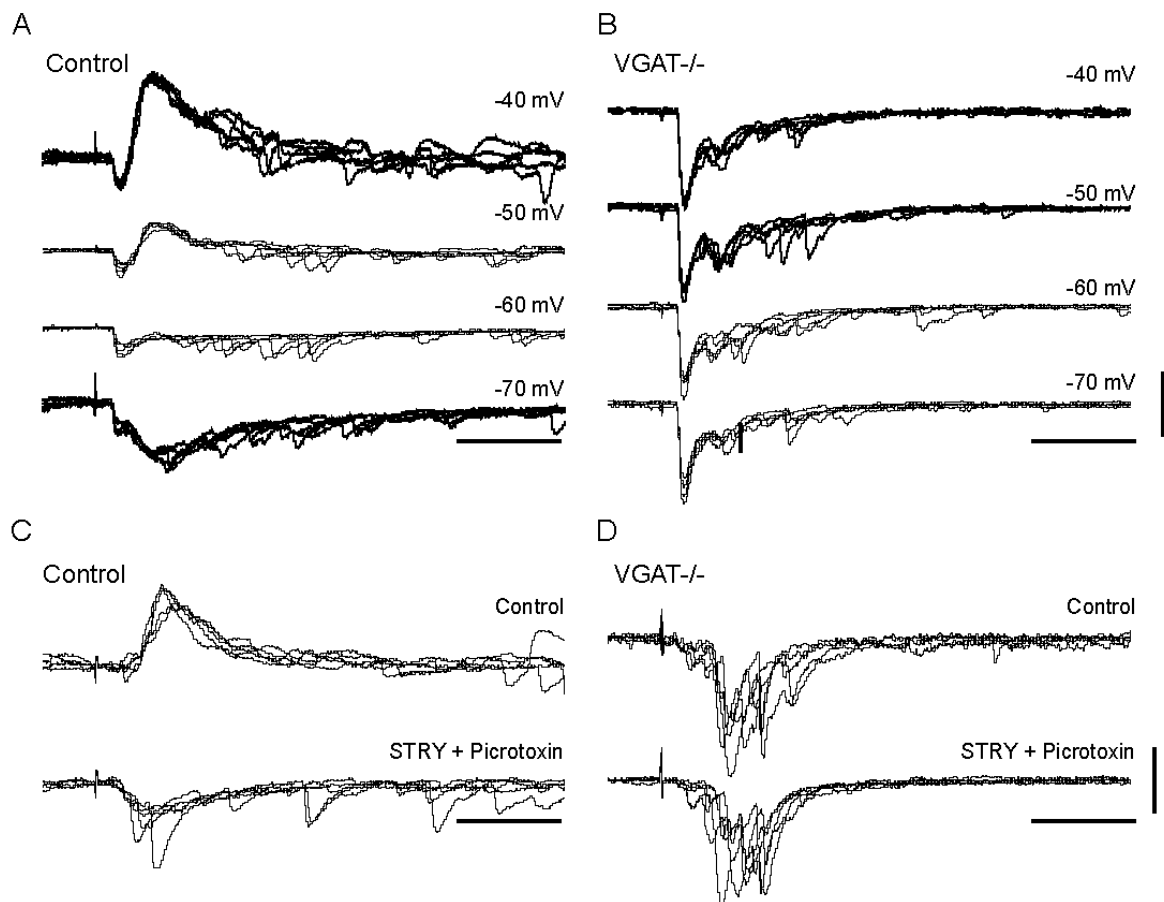


Figure 14. DR-evoked postsynaptic currents (PSCs) of MNs.

(A) DR-evoked postsynaptic currents (PSCs) of control MNs. Electrical DR stimulation evoked both inward and outward currents in control MNs under a voltage clamp.

(B) DR-evoked PSCs of VGAT^{-/-} MNs. Note that the outward currents recorded in the control were absent.

(C) The evoked outward currents in the control MNs were blocked by strychnine and picrotoxin, when the membrane potential was held at -40 mV.

(D) The antagonists of inhibitory amino acid receptors did not affect the evoked currents in VGAT^{-/-} MNs. Vertical bars indicate 100 pA (A, B), 50 pA (C, D). Horizontal bars indicate 50 ms.

6 Comparison of developmental deficits between VGAT KO and GAD67 KO mice

Cleft palate has been found in VGAT^{-/-} and GAD67^{-/-} mice (Asada et al., 1997; Condie et al., 1997; Wojcik et al., 2006), demonstrating that GABAergic transmissions are involved in palatogenesis. Because VGAT and GAD67 exhibit different molecular functions, we investigated whether the severity of cleft palate was different between VGAT^{-/-} and GAD67^{-/-} mice. Figure 15A shows hematoxylin-eosin staining of coronal sections from the oral region. In the cleft palate of VGAT^{-/-} mice, the palatal shelves remained vertical along the sides of the tongue (3 of 3). However, in GAD67^{-/-} mice, the palatal shelves elevated to a horizontal position (3 of 3). In one of the GAD67^{-/-} mice, the palatal shelves even fused (data not shown). These observations suggest that the palatogenesis progresses further in GAD67^{-/-} mice than in VGAT^{-/-} mice. Our observations also suggest that cleft palate is more severe in VGAT^{-/-} mice than GAD67^{-/-} mice.

Similar to VGAT^{-/-} mice, GAD67^{-/-} mice also had omphalocele (Figure 15B). However, the incidence was 43% (17 of 40), compared to 100% (77 of 77; see also Table 1) in VGAT^{-/-} mice. Thus, the penetrance of omphalocele was lower in GAD67^{-/-} mice. The omphalocele also appeared to be larger in VGAT^{-/-} mice. Taken together, these observations suggest that omphalocele is less severe in GAD67^{-/-} mice than VGAT^{-/-} mice, similar to what was observed with cleft palate.

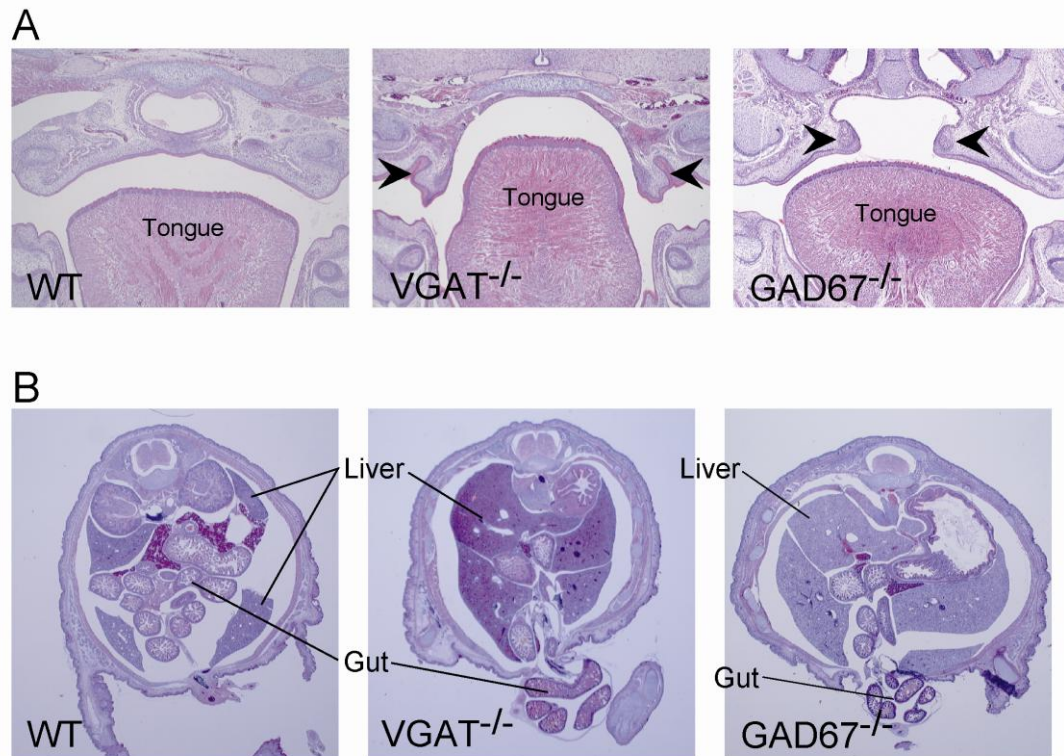


Figure 15. Histological comparison of cleft palate and omphalocele between $VGAT^{-/-}$ and $GAD67^{-/-}$ mice.

(A) Hematoxylin-eosin stained coronal sections of the oral region of E18.5 wild-type (left panel), $VGAT^{-/-}$ (middle panel), and $GAD67^{-/-}$ (right panel) mice. Histological examination revealed that the secondary palatal shelves (arrowhead) of $VGAT^{-/-}$ mice were directed vertically down along the side of the tongue in contrast to the fused palate of wild-type mice. In the cleft palate of $GAD67^{-/-}$ mice (right panel), palatal shelves failed to fuse but were elevated horizontally unlike those in $VGAT^{-/-}$ mice.

(B) Hematoxylin-eosin stained coronal sections of the umbilical region of E18.5 wild-type (left panel), $VGAT^{-/-}$ (middle panel), and $GAD67^{-/-}$ embryos (right panel). The ventral body wall of the $VGAT^{-/-}$ mice did not close and the gut protruded from the peritoneal cavity. In contrast to $VGAT^{-/-}$ mice, the ventral body wall of wild-type mice closed around the umbilicus, and the gut had already returned to the peritoneal cavity. The omphalocele was less severe in $GAD67^{-/-}$ mice than $VGAT^{-/-}$ mice because a large amount of gut was observed at the umbilical level.

DISCUSSION

The present study addresses the role of VGAT in neurotransmitter release, the occurrence of VGAT-independent release, and the contribution of VGAT to embryonic development. VGAT was found to be fundamental to the release of GABA and/or glycine in the striatum and spinal cord. The occurrence of VGAT-independent GABA release in a forebrain slice preparation. Moreover, in the absence of a vesicular transporter GABA and/or glycine, there are profound effects on muscle, liver and lung during embryonic development. These findings are important to understanding the functional roles of VGAT from the cellular to whole-body level.

Wojcik et al. (2006) generated VGAT KO mice with a mutation in exon 1, and found that they exhibited cleft palate and omphalocele. Here, I generated floxed VGAT KO mice, in which exons 2 and 3 of the VGAT gene were flanked by loxP sites. Crossing the floxed VGAT mice with CAG-Cre mice reproduced the phenotypes of cleft palate and omphalocele. Exons 1 and 2/3 encode the cytoplasmic domain and the transmembrane domain, respectively (Ebihara et al., 2003; Sagné et al., 1997). Our results demonstrate that the transmembrane domain encoded by exons 2 and 3 is indispensable to the function of VGAT.

1 Increase in overall GABA and glycine contents in VGAT^{-/-} forebrains

A few genetic studies have examined whether the loss of vesicular transporters influences levels of neurotransmitters levels in the brain. For example, monoamine levels were drastically reduced in KO mice lacking vesicular monoamine transporter 2 (VMAT2) (Wang et al., 1997), but acetylcholine levels increased in KO mice lacking vesicular acetylcholine

transporter (VACHT) compared to wild-type mice (de Castro et al., 2009). The increase in GABA levels in VGAT^{-/-} mice in the present study is similar that in ACh levels in VACHT KO mice (de Castro et al., 2009). However, in VACHT KO mice the amount of the ACh-synthesizing enzyme choline acetyltransferase (ChAT) was increased at the mRNA and protein levels compared to that in wild-type littermates, suggesting that the change in ChAT expression to be related to a compensatory mechanism due to the lack of ACh release (de Castro et al., 2009). There is no report about glutamate levels in VGluT KO mice.

The amounts of the GABA-synthesizing enzymes GAD65 and GAD67 did not differ between the VGAT^{-/-} mice and control littermates (Figure 10B, C), suggesting that the increase in GABA in the VGAT^{-/-} brain was not due to an upregulation of GAD65 and GAD67 expression. GABA and glycine are released from presynaptic neurons into the synaptic cleft and retrieved in neurons and glial cells by plasma membrane transporters (Aragón and López-Corcuera, 2003; Conti et al., 2004). The GABA and glycine taken up into glial cells are further metabolized, whereas those taken up by neurons are directly recycled into synaptic vesicles (Cherubini and Conti, 2001; Schousboe, 2003). Because the systems for degrading both GABA and glycine are mainly in glial cells (Cherubini and Conti, 2001; Sato et al., 1991) and the blocking of GABA degradation increases plasma and tissue levels (Drasbek et al., 2008; Hogema et al., 2001; Wu et al., 2006), transport into glial cells from the synaptic cleft is important for the degradation. Since no synaptic release of GABA and glycine was evident in VGAT^{-/-} mice (Figure 11A and Figure 12B), the deletion of VGAT may result in little or no transport of GABA and glycine into glial cells. Then GABA and glycine may accumulate in the GABAergic and glycinergic neurons, respectively, but they are not degraded in the glial cells of VGAT^{-/-} mice. It is worth noting that in *C.*

elegans, the mutational inactivation of VGAT led to an increase in GABA immunoreactivity in GABAergic neurons (McIntire et al., 1993). However, the presence of the extracellular GABA in VGAT^{-/-} brain (Figure 11B) does not rule out the possibility that GABA accumulate in glial cells. In addition, it is still possible that the activity, but not expression, of GAD65 and GAD67 increases in the VGAT^{-/-} brain. Further study is needed to determine the cause of the GABA increase.

2 VGAT-independent GABA release

Demarque et al. (2002) demonstrated the presence of non-vesicular (non-synaptic) GABA release by detecting GABA-receptor-mediated tonic currents recorded from immature hippocampal CA1 pyramidal neurons, which are normally synaptically silent. Because not only GABA but also β -alanine and taurine activate GABA receptors (Owens and Kriegstein, 2002a), it was important to determine whether GABA was present in the extracellular space in the VGAT^{-/-} mouse brain.

Extracellular GABA was detected in E17.5 VGAT^{-/-} forebrains and its level did not differ between VGAT^{-/-} and VGAT^{+/+} fetuses (Figure 11B). These results indicate the presence of non-vesicular GABA release in forebrain neurons. VGAT mRNA is first detected in the CNS at E10, and its expression is increased during embryonic development (Oh et al., 2005). Considering that finding together with our data, it is therefore likely that the majority of the extracellular GABA during embryonic development is derived from non-vesicular release despite the presence of VGAT. Several mechanisms of non-vesicular GABA release have been proposed. Wu et al. (2007) demonstrated that non-vesicular GABAergic neurotransmission in cultured hippocampal neurons occurs via a

reversal of the plasma membrane GABA transporter GAT-1. However, Demarque et al. (2002) did not observe a reversal of transport by GAT-1 in immature hippocampal neurons. Because our application of the GAT inhibitor nipecotic acid to forebrain slices elevated the extracellular GABA levels in both VGAT^{+/+} and VGAT^{-/-} mice, it is unlikely that reverse transport of GABA by GAT-1 plays a central role in the source of extracellular GABA in embryonic VGAT^{-/-} forebrains.

GABA_AR-mediated tonic currents, but not synaptic currents, were detected in VGAT^{-/-} striatal neurons. Considering the presence of extracellular GABA in VGAT^{-/-} brain slices, the VGAT-independent release of GABA may lead to GABA_AR-mediated tonic currents. V-ATPases power vesicular GABA accumulation, and concanamycin is its inhibitor. Rossi et al. (2003) showed that concanamycin abolished spontaneous IPSCs recorded from the cerebellar granule cells, but had no effect on tonic inhibitory currents, implying that the tonic current is activated via non-vesicular GABA release. This report supports the notion that VGAT-independent GABA release activates GABA_AR-mediated tonic currents.

3 VGAT KO mice and motor circuit formation

In the embryonic spinal cord of rodents, synaptic transmission to motoneurons mediated by GABA and glycine is prominent from the early fetal period (Hanson and Landmesser, 2003; Nishimaru et al., 1996). Furthermore, the basic neuronal pathway for the spinal reflex is formed during the prenatal period and the inhibitory connection underlies reciprocal inhibition between motoneurons innervating antagonistic muscles (Wang et al., 2008; Wu et al., 1992). The inhibitory synaptic transmission onto motoneurons was clearly absent in the spinal motoneurons, suggesting the absence of other functional

mechanisms that transport GABA and/or glycine into SVs in these synapses. VGAT^{-/-} fetuses at E17.5-18.5 not only were completely immobile and stiff, but did not respond to mechanical stimuli by pinching of the tail. Therefore, the lack of inhibitory transmission onto motoneurons in VGAT^{-/-} fetuses probably resulted in defects in spontaneous and stimulus-induced movements *in vivo*.

Despite the clear absence of inhibitory neurotransmission and impaired motor function, excitatory connections mediating sensory inputs to motoneurons formed in the VGAT^{-/-} spinal cord and were capable of transmitting sensory information from the primary afferents. There is increasing evidence that GABA has a trophic role in neural development (Behar et al., 1996; Ganguly et al., 2001; Owens and Kriegstein, 2002b; Represa and Ben-Ari, 2005; Varju et al., 2001). In contrast, blocking GABAergic and glycinergic transmission in spinal cord explants from rat embryos had little effect on the differentiation of the membrane properties of motoneurons (Xie and Ziskind-Conhaim, 1995). Inhibitory neurotransmission may not be indispensable to the circuit formation. Since the present results do not imply that the excitatory synapses in the VGAT^{-/-} spinal cord are as developed as those in the control spinal cord, further study is needed to establish the involvement of GABAergic and glycinergic signaling in neural circuit formation.

4 Differences in phenotypic severity between GAD67^{-/-} and VGAT^{-/-} mice

The more severe defects in VGAT KO mice are consistent with the notion of residual neurotransmission in GAD67 KO mice. Glycinergic transmission is present in embryonic spinal cord and brainstem (Greer and Funk, 2005).

Hyperekplexia is a neurogenetic disorder caused mostly by mutations in the gene encoding the $\alpha 1$ subunit of the glycine receptor and is characterized by an exaggerated startle response and neonatal hypertonia. In patients with hyperekplexia, the recurrent abdominal muscle contraction caused by the exaggerated startle response can increase abdominal pressure and lead to omphalocele and inguinal hernia (Suhren et al., 1966; Zhou et al., 2002). A defect in glycinergic transmission might be involved in the onset of omphalocele, even though a small amount of GABA is synthesized by GAD65 at the embryonic stage (Asada et al., 1997; Ji et al., 1999). The differences in severity between VGAT^{-/-} and GAD67^{-/-} mice would be due to the presence of both glycinergic and GAD65-produced GABAergic transmission in GAD67^{-/-} fetuses, but not in VGAT^{-/-} fetuses.

5 Developmental defects of non-neural tissues in mice with impaired inhibitory neurotransmission

In addition to the defect in motor movement, trapezius muscle displayed atrophy in VGAT^{-/-} mice. Embryonic myogenesis progresses via the proliferation of myoblasts and fusion of myotubes, but also requires substantial cell death (Sandri and Carraro, 1999). Physical stimuli play a significant role in the development and maintenance of skeletal muscle (Proske and Morgan, 2001). In cultured myoblasts, chronic and cyclic stretching result in an increase in cell death, including apoptosis (Liu et al., 2009). Therefore, a possible explanation for the atrophy in VGAT^{-/-} trapezius muscle is that the muscle was stretched due to the hunched posture and caused an increase in apoptosis during development.

Defects in ventral body wall closure, such as omphalocele, are common human birth defects, but their molecular and cellular bases are poorly understood

(Williams, 2008). The mouse provides a model to study the genetic defects and environmental insults that can lead to defects of ventral body wall closure (Brewer and Williams, 2004). In this study, omphalocele was observed in both VGAT^{-/-} and GAD67^{-/-} mice, indicating that lack of GABA signaling was involved in its onset. A hunched posture due to the lack of inhibitory transmission would result in increases in both intrathoracic and intraabdominal pressure which may disturb the gut return to the peritoneal cavity.

The present study extended our knowledge of the role of VGAT in embryonic development with new findings of defects in muscle, liver, and lung, even though the cleft palate and omphalocele in VGAT^{-/-} mice have been reported previously (Oh et al., 2010; Wojcik et al., 2006). The developmental defects seen in the present study and others seem to be secondary to the loss of inhibitory neurotransmission. Evidence supporting this view includes the palatal formation of GAD67^{-/-} and VGAT^{-/-} cultured palatal explants. Iseki et al. (2007) reported that explants dissected from GAD67^{-/-} embryos could undergo palatal fusion. Oh et al. (2010) obtained similar results in different lines of GAD67^{-/-} and VGAT^{-/-} mice. These reports suggest that the potential for palatogenesis is preserved in palatal shelves despite the impaired inhibitory neurotransmission.

VGAT^{-/-} fetuses are immobile, stiff, and unresponsive to mechanical stimuli. Tsunekawa et al. (2005) also reported that movements of the tongue and mouth are impaired in GAD67^{-/-} fetuses. Fetal movement is a precondition for normal development and growth. Limitations of movement, regardless of the underlying causes, can result in a particular pattern of abnormal fetal morphogenesis (Hall, 2009). For example, fetal movement suggests a role in muscle and joint development (Pitsillides, 2006), bone formation (Archer et al., 2003). In addition to the skeletal system, the lung also requires mechanical

stimuli for their development (Tseng et al., 2000). Taken together, it seems possible that the developmental defects in VGAT^{-/-} mice result from a failure of developmental processes that involve fetal movement.

CONCLUSION

Primary achievement of this study was to establish VGAT KO mice, with which I demonstrated that VGAT is fundamental to GABAergic and/or glycinergic neurotransmission.

This study provides a wide variety of evidences that VGAT is vital for embryonic development. The multiple developmental defects seen in VGAT^{-/-} mice indicate that VGAT is essential not only in inhibitory neurotransmission but also in tissue development.

The presence of extracellular GABA in the VGAT^{-/-} forebrain suggests that GABA to be released by non-vesicular mechanism. Moreover, the comparable value to the wild type indicates that this form of release may account for the majority of extracellular GABA in the developing brain.

In the absence of synaptic inhibition, the excitatory connections mediating sensory inputs to motoneurons were formed in the VGAT^{-/-} spinal cord and were capable of transmitting sensory information from the primary afferents. Inhibitory neurotransmission might not be indispensable to the circuit formation.

Recent progress in the study with inhibitory neurotransmission has elucidated that the inhibitory system has a substantial complex mechanism of action. The conditional VGAT mice described here may provide a useful tool for the study of specific functions of VGAT-dependent GABAergic and/or glycinergic transmission. For example, GABAergic neurons are classified into subtypes according to the expression of chemical markers such as parvalbumin and somatostatin. Therefore, conditional VGAT mice will be useful for investigating the role of VGAT in GABAergic neuronal subtypes.

ACKNOWLEDGEMENTS

First of all, I would like to express my deepest thanks to Prof. Yuchio Yanagawa who took me into his group. Prof. Yanagawa has shown great kindness and patience in helping me over the years.

Special thanks are also due to Dr. Toshikazu Kakizaki, who encouraged me continuously and provided valuable training and suggestions to improve my thesis.

I want to thank Dr. Hiroshi Nishimaru for his collaborative work and valuable discussions. Without his patience and scientific advice, I would not have been able to finish my study.

I wish to express my warm thanks to Dr. Tomonori Furukawa, Prof. Atsuo Fukuda, Dr. Ryotaro Hayashi, and Prof. Manabu Fukumoto for their excellent collaborative work and helpful discussions.

I want to thank Prof. Shigeo Takamori who gave me the opportunity to learn his progressive experimental skills. This was a worthwhile experience especially at the beginning of graduate school.

I thank Ms. Honma, Ms. Hara and Ms. Yamazaki for technical assistance, and Ms. Shimoda and Ms. Owada for secretarial assistance. I thank Drs. Iso and Kurabayashi for helping with the experiments and discussions. I also thank the staff at the Institute of Experimental Animal Research, Gunma University Graduate School of Medicine for technical help.

During my research I have collaborated with colleagues for whom I have great regard, and I wish to extend my warmest thanks to all those who have helped me, especially Yoichi Nakazato, Satoe Ebihara, Masakazu Uematsu, Masayoshi Mishina, Jun-ichi Miyazaki, Minesuke Yokoyama, Shiro Konishi, Koichi Inoue, Kenji Nakamura, and Kunihiro Obata

Finally, I would like to thank my parents for their love and forgiveness, and my sister, Yuko, for bringing me endless happiness.

REFERENCES

- Ade, K. K., Janssen, M. J., Ortinski, P. I., and Vicini, S. (2008). Differential tonic GABA conductances in striatal medium spiny neurons. *J Neurosci* 28, 1185-1197.
- Aragón, C., and López-Corcuera, B. (2003). Structure, function and regulation of glycine neurotransmitters. *Eur J Pharmacol* 479, 249-262.
- Archer, C. W., Dowthwaite, G. P., and Francis-West, P. (2003). Development of synovial joints. *Birth Defects Res C Embryo Today* 69, 144-155.
- Asada, H., Kawamura, Y., Maruyama, K., Kume, H., Ding, R., Ji, F. Y., Kanbara, N., Kuzume, H., Sanbo, M., Yagi, T., and Obata, K. (1996). Mice lacking the 65 kDa isoform of glutamic acid decarboxylase (GAD65) maintain normal levels of GAD67 and GABA in their brains but are susceptible to seizures. *Biochem Biophys Res Commun* 229, 891-895.
- Asada, H., Kawamura, Y., Maruyama, K., Kume, H., Ding, R. G., Kanbara, N., Kuzume, H., Sanbo, M., Yagi, T., and Obata, K. (1997). Cleft palate and decreased brain gamma-aminobutyric acid in mice lacking the 67-kDa isoform of glutamic acid decarboxylase. *Proc Natl Acad Sci USA* 94, 6496-6499.
- Attwell, D., Barbour, B., and Szatkowski, M. (1993). Nonvesicular release of neurotransmitter. *Neuron* 11, 401-407.
- Baertschi, S., Zhuang, L., and Trueb, B. (2007). Mice with a targeted disruption of the *Fgfr1* gene die at birth due to alterations in the diaphragm. *FEBS J* 274, 6241-6253.
- Bak, L. K., Schousboe, A., and Waagepetersen, H. S. (2006). The glutamate/GABA-glutamine cycle: aspects of transport, neurotransmitter homeostasis and ammonia transfer. *J Neurochem* 98, 641-653.
- Behar, T. N., Li, Y. X., Tran, H. T., Ma, W., Dunlap, V., Scott, C., and Barker, J. L. (1996). GABA stimulates chemotaxis and chemokinesis of embryonic cortical neurons via calcium-dependent mechanisms. *J Neurosci* 16, 1808-1818.
- Bellocchio, E. E., Reimer, R. J., Fremeau, R. T., Jr., and Edwards, R. H. (2000). Uptake of glutamate into synaptic vesicles by an inorganic phosphate transporter. *Science* 289, 957-960.
- Ben-Ari, Y. (2002). Excitatory actions of gaba during development: the nature of the nurture. *Nat Rev Neurosci* 3, 728-739.
- Blankenship, A. G., and Feller, M. B. (2010). Mechanisms underlying spontaneous patterned activity in developing neural circuits. *Nat Rev Neurosci* 11, 18-29.
- Boehm, S. L., 2nd, Ponomarev, I., Jennings, A. W., Whiting, P. J., Rosahl, T. W., Garrett, E. M., Blednov, Y. A., and Harris, R. A. (2004). gamma-Aminobutyric acid A receptor subunit mutant mice: new

perspectives on alcohol actions. *Biochem Pharmacol* 68, 1581-1602.

Bolam, J. P., Hanley, J. J., Booth, P. A., and Bevan, M. D. (2000). Synaptic organisation of the basal ganglia. *J Anat* 196 (Pt 4), 527-542.

Brewer, S., and Williams, T. (2004). Finally, a sense of closure? Animal models of human ventral body wall defects. *Bioessays* 26, 1307-1321.

Brickley, S. G., Cull-Candy, S. G., and Farrant, M. (1996). Development of a tonic form of synaptic inhibition in rat cerebellar granule cells resulting from persistent activation of GABAA receptors. *J Physiol* 497 (Pt 3), 753-759.

Chadderton, P., Margrie, T. W., and Hausser, M. (2004). Integration of quanta in cerebellar granule cells during sensory processing. *Nature* 428, 856-860.

Chaudhry, F. A., Reimer, R. J., Bellocchio, E. E., Danbolt, N. C., Osen, K. K., Edwards, R. H., and Storm-Mathisen, J. (1998). The vesicular GABA transporter, VGAT, localizes to synaptic vesicles in sets of glycinergic as well as GABAergic neurons. *J Neurosci* 18, 9733-9750.

Cherubini, E., and Conti, F. (2001). Generating diversity at GABAergic synapses. *Trends Neurosci* 24, 155-162.

Chessler, S. D., Simonson, W. T., Sweet, I. R., and Hammerle, L. P. (2002). Expression of the vesicular inhibitory amino acid transporter in pancreatic islet cells: distribution of the transporter within rat islets. *Diabetes* 51, 1763-1771.

Condie, B. G., Bain, G., Gottlieb, D. I., and Capecchi, M. R. (1997). Cleft palate in mice with a targeted mutation in the gamma-aminobutyric acid-producing enzyme glutamic acid decarboxylase 67. *Proc Natl Acad Sci USA* 94, 11451-11455.

Conti, F., Minelli, A., and Melone, M. (2004). GABA transporters in the mammalian cerebral cortex: localization, development and pathological implications. *Brain Res Brain Res Rev* 45, 196-212.

Dalby, N. O. (2003). Inhibition of gamma-aminobutyric acid uptake: anatomy, physiology and effects against epileptic seizures. *Eur J Pharmacol* 479, 127-137.

de Castro, B. M., De Jaeger, X., Martins-Silva, C., Lima, R. D., Amaral, E., Menezes, C., Lima, P., Neves, C. M., Pires, R. G., Gould, T. W., *et al.* (2009). The vesicular acetylcholine transporter is required for neuromuscular development and function. *Mol Cell Biol* 29, 5238-5250.

DeLong, M. R. (1990). Primate models of movement disorders of basal ganglia origin. *Trends Neurosci* 13, 281-285.

Delpire, E. (2000). Cation-Chloride Cotransporters in Neuronal Communication. *News Physiol Sci* 15, 309-312.

- Demarque, M., Represa, A., Becq, H., Khalilov, I., Ben-Ari, Y., and Aniksztejn, L. (2002). Paracrine intercellular communication by a Ca²⁺- and SNARE-independent release of GABA and glutamate prior to synapse formation. *Neuron* 36, 1051-1061.
- Drasbek, K. R., Vardya, I., Delenclos, M., Gibson, K. M., and Jensen, K. (2008). SSADH deficiency leads to elevated extracellular GABA levels and increased GABAergic neurotransmission in the mouse cerebral cortex. *J Inherit Metab Dis* 31, 662-668.
- Dumoulin, A., Rostaing, P., Bedet, C., Lévi, S., Isambert, M. F., Henry, J. P., Triller, A., and Gasnier, B. (1999). Presence of the vesicular inhibitory amino acid transporter in GABAergic and glycinergic synaptic terminal boutons. *J Cell Sci* 112, 811-823.
- Ebihara, S., Obata, K., and Yanagawa, Y. (2003). Mouse vesicular GABA transporter gene: genomic organization, transcriptional regulation and chromosomal localization. *Brain Res Mol Brain Res* 110, 126-139.
- Ehrlich, I., Lohrke, S., and Friauf, E. (1999). Shift from depolarizing to hyperpolarizing glycine action in rat auditory neurones is due to age-dependent Cl⁻ regulation. *J Physiol* 520 Pt 1, 121-137.
- Farrant, M., and Nusser, Z. (2005). Variations on an inhibitory theme: phasic and tonic activation of GABA(A) receptors. *Nat Rev Neurosci* 6, 215-229.
- Fritschy, J. M., Paysan, J., Enna, A., and Mohler, H. (1994). Switch in the expression of rat GABA_A-receptor subtypes during postnatal development: an immunohistochemical study. *J Neurosci* 14, 5302-5324.
- Fujii, M., Arata, A., Kanbara-Kume, N., Saito, K., Yanagawa, Y., and Obata, K. (2007). Respiratory activity in brainstem of fetal mice lacking glutamate decarboxylase 65/67 and vesicular GABA transporter. *Neuroscience* 146, 1044-1052.
- Ganguly, K., Schinder, A. F., Wong, S. T., and Poo, M. (2001). GABA itself promotes the developmental switch of neuronal GABAergic responses from excitation to inhibition. *Cell* 105, 521-532.
- Gao, B. X., and Ziskind-Conhaim, L. (1995). Development of glycine- and GABA-gated currents in rat spinal motoneurons. *J Neurophysiol* 74, 113-121.
- Geigerseder, C., Doepner, R., Thalhammer, A., Frungieri, M. B., Gamel-Didelon, K., Calandra, R. S., Kohn, F. M., and Mayerhofer, A. (2003). Evidence for a GABAergic system in rodent and human testis: local GABA production and GABA receptors. *Neuroendocrinology* 77, 314-323.
- Glykys, J., and Mody, I. (2007). Activation of GABA_A receptors: views from outside the synaptic cleft. *Neuron* 56, 763-770.
- Gomez, J., Ohno, K., Hulsmann, S., Armsen, W., Eulenburg, V., Richter, D. W., Laube, B., and Betz, A. (2007). The GABA_A receptor $\alpha 6$ subunit is essential for the development of the mouse cerebellum. *J Neurosci* 27, 1151-1161.

- H. (2003). Deletion of the mouse glycine transporter 2 results in a hyperekplexia phenotype and postnatal lethality. *Neuron* 40, 797-806.
- Greer, J. J., and Funk, G. D. (2005). Perinatal development of respiratory motoneurons. *Respir Physiol Neurobiol* 149, 43-61.
- Grillner, S., Hellgren, J., Menard, A., Saitoh, K., and Wikstrom, M. A. (2005). Mechanisms for selection of basic motor programs--roles for the striatum and pallidum. *Trends Neurosci* 28, 364-370.
- Hall, J. G. (2009). Pena-Shokeir phenotype (fetal akinesia deformation sequence) revisited. *Birth Defects Res A Clin Mol Teratol* 85, 677-694.
- Hamann, M., Rossi, D. J., and Attwell, D. (2002). Tonic and spillover inhibition of granule cells control information flow through cerebellar cortex. *Neuron* 33, 625-633.
- Hanson, M. G., and Landmesser, L. T. (2003). Characterization of the circuits that generate spontaneous episodes of activity in the early embryonic mouse spinal cord. *J Neurosci* 23, 587-600.
- Hashiguti, H., Nakahara, D., Maruyama, W., Naoi, M., and Ikeda, T. (1993). Simultaneous determination of in vivo hydroxylation of tyrosine and tryptophan in rat striatum by microdialysis-HPLC: relationship between dopamine and serotonin biosynthesis. *J Neural Transm Gen Sect* 93, 213-223.
- Hayashi, M., Otsuka, M., Morimoto, R., Muroyama, A., Uehara, S., Yamamoto, A., and Moriyama, Y. (2003). Vesicular inhibitory amino acid transporter is present in glucagon-containing secretory granules in alphaTC6 cells, mouse clonal alpha-cells, and alpha-cells of islets of Langerhans. *Diabetes* 52, 2066-2074.
- Hell, J. W., Edelmann, L., Hartinger, J., and Jahn, R. (1991). Functional reconstitution of the gamma-aminobutyric acid transporter from synaptic vesicles using artificial ion gradients. *Biochemistry* 30, 11795-11800.
- Hell, J. W., Maycox, P. R., and Jahn, R. (1990). Energy dependence and functional reconstitution of the gamma-aminobutyric acid carrier from synaptic vesicles. *J Biol Chem* 265, 2111-2117.
- Hogema, B. M., Gupta, M., Senephansiri, H., Burlingame, T. G., Taylor, M., Jakobs, C., Schutgens, R. B., Froestl, W., Snead, O. C., Diaz-Arrastia, R., *et al.* (2001). Pharmacologic rescue of lethal seizures in mice deficient in succinate semialdehyde dehydrogenase. *Nat Genet* 29, 212-216.
- Homanics, G. E., DeLorey, T. M., Firestone, L. L., Quinlan, J. J., Handforth, A., Harrison, N. L., Krasowski, M. D., Rick, C. E., Korpi, E. R., Makela, R., *et al.* (1997). Mice devoid of gamma-aminobutyrate type A receptor beta3 subunit have epilepsy, cleft palate, and hypersensitive behavior. *Proc Natl Acad Sci USA* 94, 4143-4148.
- Hübner, C. A., Stein, V., Hermans-Borgmeyer, I., Meyer, T., Ballanyi, K., and Jentsch, T. J. (2001).

Disruption of KCC2 reveals an essential role of K-Cl cotransport already in early synaptic inhibition. *Neuron* 30, 515-524.

Iseki, S., Ishii-Suzuki, M., Tsunekawa, N., Yamada, Y., Eto, K., and Obata, K. (2007). Experimental induction of palate shelf elevation in glutamate decarboxylase 67-deficient mice with cleft palate due to vertically oriented palatal shelf. *Birth Defects Res A Clin Mol Teratol* 79, 688-695.

Jensen, K., Chiu, C. S., Sokolova, I., Lester, H. A., and Mody, I. (2003). GABA transporter-1 (GAT1)-deficient mice: differential tonic activation of GABA_A versus GABA_B receptors in the hippocampus. *J Neurophysiol* 90, 2690-2701.

Ji, F., Kanbara, N., and Obata, K. (1999). GABA and histogenesis in fetal and neonatal mouse brain lacking both the isoforms of glutamic acid decarboxylase. *Neurosci Res* 33, 187-194.

Jonas, P., Bischofberger, J., and Sandkuhler, J. (1998). Corelease of two fast neurotransmitters at a central synapse. *Science* 281, 419-424.

Juge, N., Muroyama, A., Hiasa, M., Omote, H., and Moriyama, Y. (2009). Vesicular inhibitory amino acid transporter is a Cl⁻/gamma-aminobutyrate Co-transporter. *J Biol Chem* 284, 35073-35078.

Kandler, K., Kullmann, P. H., Ene, F. A., and Kim, G. (2002). Excitatory action of an immature glycinergic/GABAergic sound localization pathway. *Physiol Behav* 77, 583-587.

Kaneda, M., Farrant, M., and Cull-Candy, S. G. (1995). Whole-cell and single-channel currents activated by GABA and glycine in granule cells of the rat cerebellum. *J Physiol* 485 (Pt 2), 419-435.

Kaneko, K., Tamamaki, N., Owada, H., Kakizaki, T., Kume, N., Totsuka, M., Yamamoto, T., Yawo, H., Yagi, T., Obata, K., and Yanagawa, Y. (2008). Noradrenergic excitation of a subpopulation of GABAergic cells in the basolateral amygdala via both activation of nonselective cationic conductance and suppression of resting K⁺ conductance: a study using glutamate decarboxylase 67-green fluorescent protein knock-in mice. *Neuroscience* 157, 781-797.

Kanner, B. I. (2006). Structure and function of sodium-coupled GABA and glutamate transporters. *J Membr Biol* 213, 89-100.

Kash, S. F., Johnson, R. S., Tecott, L. H., Noebels, J. L., Mayfield, R. D., Hanahan, D., and Baekkeskov, S. (1997). Epilepsy in mice deficient in the 65-kDa isoform of glutamic acid decarboxylase. *Proc Natl Acad Sci U S A* 94, 14060-14065.

Kish, P. E., Fischer-Bovenkerk, C., and Ueda, T. (1989). Active transport of gamma-aminobutyric acid and glycine into synaptic vesicles. *Proc Natl Acad Sci USA* 86, 3877-3881.

Kishioka, A., Fukushima, F., Ito, T., Kataoka, H., Mori, H., Ikeda, T., Itohara, S., Sakimura, K., and Mishina, M. (2009). A novel form of memory for auditory fear conditioning at a low-intensity

unconditioned stimulus. PLoS One 4, e4157.

Kotak, V. C., Korada, S., Schwartz, I. R., and Sanes, D. H. (1998). A developmental shift from GABAergic to glycinergic transmission in the central auditory system. *J Neurosci* 18, 4646-4655.

Kudo, N., and Yamada, T. (1987). Morphological and physiological studies of development of the monosynaptic reflex pathway in the rat lumbar spinal cord. *J Physiol* 389, 441-459.

Laurie, D. J., Wisden, W., and Seeburg, P. H. (1992). The distribution of thirteen GABAA receptor subunit mRNAs in the rat brain. III. Embryonic and postnatal development. *J Neurosci* 12, 4151-4172.

Liu, J., Liu, J., Mao, J., Yuan, X., Lin, Z., and Li, Y. (2009). Caspase-3-mediated cyclic stretch-induced myoblast apoptosis via a Fas/FasL-independent signaling pathway during myogenesis. *J Cell Biochem* 107, 834-844.

Liu, Z., Neff, R. A., and Berg, D. K. (2006). Sequential interplay of nicotinic and GABAergic signaling guides neuronal development. *Science* 314, 1610-1613.

Lu, C. C., and Hilgemann, D. W. (1999). GAT1 (GABA:Na⁺:Cl⁻) cotransport function. Steady state studies in giant *Xenopus* oocyte membrane patches. *J Gen Physiol* 114, 429-444.

Maguire, J. L., Stell, B. M., Rafizadeh, M., and Mody, I. (2005). Ovarian cycle-linked changes in GABA(A) receptors mediating tonic inhibition alter seizure susceptibility and anxiety. *Nat Neurosci* 8, 797-804.

Martens, H., Weston, M. C., Boulland, J. L., Gronborg, M., Grosche, J., Kacza, J., Hoffmann, A., Matteoli, M., Takamori, S., Harkany, T., *et al.* (2008). Unique luminal localization of VGAT-C terminus allows for selective labeling of active cortical GABAergic synapses. *J Neurosci* 28, 13125-13131.

Mayerhofer, A., Hohne-Zell, B., Gamel-Didelon, K., Jung, H., Redecker, P., Grube, D., Urbanski, H. F., Gasnier, B., Fritschy, J. M., and Gratzl, M. (2001). Gamma-aminobutyric acid (GABA): a para- and/or autocrine hormone in the pituitary. *Faseb J* 15, 1089-1091.

McIntire, S. L., Jorgensen, E., and Horvitz, H. R. (1993). Genes required for GABA function in *Caenorhabditis elegans*. *Nature* 364, 334-337.

McIntire, S. L., Reimer, R. J., Schuske, K., Edwards, R. H., and Jorgensen, E. M. (1997). Identification and characterization of the vesicular GABA transporter. *Nature* 389, 870-876.

Miller, R. P., and Becker, B. A. (1975). Teratogenicity of oral diazepam and diphenylhydantoin in mice. *Toxicol Appl Pharmacol* 32, 53-61.

Minelli, A., Alonso-Nanclares, L., Edwards, R. H., DeFelipe, J., and Conti, F. (2003). Postnatal development of the vesicular GABA transporter in rat cerebral cortex. *Neuroscience* 117, 337-346.

- Nabekura, J., Katsurabayashi, S., Kakazu, Y., Shibata, S., Matsubara, A., Jinno, S., Mizoguchi, Y., Sasaki, A., and Ishibashi, H. (2004). Developmental switch from GABA to glycine release in single central synaptic terminals. *Nat Neurosci* 7, 17-23.
- Nakahara, D., Nakamura, M., Iigo, M., and Okamura, H. (2003). Bimodal circadian secretion of melatonin from the pineal gland in a living CBA mouse. *Proc Natl Acad Sci USA* 100, 9584-9589.
- Nishimaru, H., Iizuka, M., Ozaki, S., and Kudo, N. (1996). Spontaneous motoneuronal activity mediated by glycine and GABA in the spinal cord of rat fetuses in vitro. *J Physiol* 497, 131-143.
- Nishimaru, H., Restrepo, C. E., Ryge, J., Yanagawa, Y., and Kiehn, O. (2005). Mammalian motor neurons corelease glutamate and acetylcholine at central synapses. *Proc Natl Acad Sci USA* 102, 5245-5249.
- Oh, W. J., Noggle, S. A., Maddox, D. M., and Condie, B. G. (2005). The mouse vesicular inhibitory amino acid transporter gene: expression during embryogenesis, analysis of its core promoter in neural stem cells and a reconsideration of its alternate splicing. *Gene* 351, 39-49.
- Oh, W. J., Westmoreland, J. J., Summers, R., and Condie, B. G. (2010). Cleft palate is caused by CNS dysfunction in *Gad1* and *Viaat* knockout mice. *PLoS One* 5, e9758.
- Olah, S., Fule, M., Komlosi, G., Varga, C., Baldi, R., Barzo, P., and Tamas, G. (2009). Regulation of cortical microcircuits by unitary GABA-mediated volume transmission. *Nature* 461, 1278-1281.
- Owens, D. F., Boyce, L. H., Davis, M. B., and Kriegstein, A. R. (1996). Excitatory GABA responses in embryonic and neonatal cortical slices demonstrated by gramicidin perforated-patch recordings and calcium imaging. *J Neurosci* 16, 6414-6423.
- Owens, D. F., and Kriegstein, A. R. (2002a). Developmental neurotransmitters? *Neuron* 36, 989-991.
- Owens, D. F., and Kriegstein, A. R. (2002b). Is there more to GABA than synaptic inhibition? *Nat Rev Neurosci* 3, 715-727.
- Peason, K., and Gordon, J. (2000). Spinal reflex. In *Principles of Neural Science*, 4th ed., E. R. Kandel, J. H. Schwartz, and T. M. Jessell, eds. (New York, McGraw-Hill), pp. 713-736.
- Pirker, S., Schwarzer, C., Wieselthaler, A., Sieghart, W., and Sperk, G. (2000). GABA(A) receptors: immunocytochemical distribution of 13 subunits in the adult rat brain. *Neuroscience* 101, 815-850.
- Pitsillides, A. A. (2006). Early effects of embryonic movement: 'a shot out of the dark'. *J Anat* 208, 417-431.
- Proske, U., and Morgan, D. L. (2001). Muscle damage from eccentric exercise: mechanism, mechanical signs, adaptation and clinical applications. *J Physiol* 537, 333-345.

- Represa, A., and Ben-Ari, Y. (2005). Trophic actions of GABA on neuronal development. *Trends Neurosci* 28, 278-283.
- Rossi, D. J., Hamann, M., and Attwell, D. (2003). Multiple modes of GABAergic inhibition of rat cerebellar granule cells. *J Physiol* 548, 97-110.
- Sagné, C., El Mestikawy, S., Isambert, M. F., Hamon, M., Henry, J. P., Giros, B., and Gasnier, B. (1997). Cloning of a functional vesicular GABA and glycine transporter by screening of genome databases. *FEBS Lett* 417, 177-183.
- Sakai, K., and Miyazaki, J. (1997). A transgenic mouse line that retains Cre recombinase activity in mature oocytes irrespective of the cre transgene transmission. *Biochem Biophys Res Commun* 237, 318-324.
- Sandri, M., and Carraro, U. (1999). Apoptosis of skeletal muscles during development and disease. *Int J Biochem Cell Biol* 31, 1373-1390.
- Sato, K., Yoshida, S., Fujiwara, K., Tada, K., and Tohyama, M. (1991). Glycine cleavage system in astrocytes. *Brain Res* 567, 64-70.
- Schousboe, A. (2003). Role of astrocytes in the maintenance and modulation of glutamatergic and GABAergic neurotransmission. *Neurochem Res* 28, 347-352.
- Semyanov, A., Walker, M. C., and Kullmann, D. M. (2003). GABA uptake regulates cortical excitability via cell type-specific tonic inhibition. *Nat Neurosci* 6, 484-490.
- Singer, J. H., Talley, E. M., Bayliss, D. A., and Berger, A. J. (1998). Development of glycinergic synaptic transmission to rat brain stem motoneurons. *J Neurophysiol* 80, 2608-2620.
- Stein, V., and Nicoll, R. A. (2003). GABA generates excitement. *Neuron* 37, 375-378.
- Stell, B. M., and Mody, I. (2002). Receptors with different affinities mediate phasic and tonic GABA(A) conductances in hippocampal neurons. *J Neurosci* 22, RC223.
- Suhren, O., Bruyn, G. W., and Tuynman, J. A. (1966). Hyperexplexia - A Hereditary Startle Syndrome. *J Neurol Sci* 3, 577-605.
- Supplisson, S., and Roux, M. J. (2002). Why glycine transporters have different stoichiometries. *FEBS Lett* 529, 93-101.
- Takamori, S., Rhee, J. S., Rosenmund, C., and Jahn, R. (2000a). Identification of a vesicular glutamate transporter that defines a glutamatergic phenotype in neurons. *Nature* 407, 189-194.
- Takamori, S., Riedel, D., and Jahn, R. (2000b). Immunolocalization of GABA-specific synaptic vesicles defines a functionally distinct subset of synaptic vesicles. *J Neurosci* 20, 4904-4911.

- Tamamaki, N., Yanagawa, Y., Tomioka, R., Miyazaki, J., Obata, K., and Kaneko, T. (2003). Green fluorescent protein expression and colocalization with calretinin, parvalbumin, and somatostatin in the GAD67-GFP knock-in mouse. *J Comp Neurol* 467, 60-79.
- Tapia, J. C., Mentis, G. Z., Navarrete, R., Nualart, F., Figueroa, E., Sanchez, A., and Aguayo, L. G. (2001). Early expression of glycine and GABA(A) receptors in developing spinal cord neurons. Effects on neurite outgrowth. *Neuroscience* 108, 493-506.
- Tocco, D. R., Renskers, K., and Zimmerman, E. F. (1987). Diazepam-induced cleft palate in the mouse and lack of correlation with the H-2 locus. *Teratology* 35, 439-445.
- Tseng, B. S., Cavin, S. T., Booth, F. W., Olson, E. N., Marin, M. C., McDonnell, T. J., and Butler, I. J. (2000). Pulmonary hypoplasia in the myogenin null mouse embryo. *Am J Respir Cell Mol Biol* 22, 304-315.
- Tsunekawa, N., Arata, A., and Obata, K. (2005). Development of spontaneous mouth/tongue movement and related neural activity, and their repression in fetal mice lacking glutamate decarboxylase 67. *Eur J Neurosci* 21, 173-178.
- Varju, P., Katarova, Z., Madarasz, E., and Szabo, G. (2001). GABA signalling during development: new data and old questions. *Cell Tissue Res* 305, 239-246.
- Varoqui, H., and Erickson, J. D. (1996). Active transport of acetylcholine by the human vesicular acetylcholine transporter. *J Biol Chem* 271, 27229-27232.
- Vicini, S., and Ortinski, P. (2004). Genetic manipulations of GABAA receptor in mice make inhibition exciting. *Pharmacol Ther* 103, 109-120.
- Wall, M. J., and Usowicz, M. M. (1997). Development of action potential-dependent and independent spontaneous GABAA receptor-mediated currents in granule cells of postnatal rat cerebellum. *Eur J Neurosci* 9, 533-548.
- Wang, Q., Jolly, J. P., Surmeier, J. D., Mullah, B. M., Lidow, M. S., Bergson, C. M., and Robishaw, J. D. (2001). Differential dependence of the D1 and D5 dopamine receptors on the G protein gamma 7 subunit for activation of adenylylcyclase. *J Biol Chem* 276, 39386-39393.
- Wang, Y. M., Gainetdinov, R. R., Fumagalli, F., Xu, F., Jones, S. R., Bock, C. B., Miller, G. W., Wightman, R. M., and Caron, M. G. (1997). Knockout of the vesicular monoamine transporter 2 gene results in neonatal death and supersensitivity to cocaine and amphetamine. *Neuron* 19, 1285-1296.
- Wang, Z., Li, L., Goulding, M., and Frank, E. (2008). Early postnatal development of reciprocal Ia inhibition in the murine spinal cord. *J Neurophysiol* 100, 185-196.
- Watson, J. B., Coulter, P. M., 2nd, Margulies, J. E., de Lecea, L., Danielson, P. E., Erlander, M. G., and

- Sutcliffe, J. G. (1994). G-protein gamma 7 subunit is selectively expressed in medium-sized neurons and dendrites of the rat neostriatum. *J Neurosci Res* 39, 108-116.
- Wee, E. L., and Zimmerman, E. F. (1983). Involvement of GABA in palate morphogenesis and its relation to diazepam teratogenesis in two mouse strains. *Teratology* 28, 15-22.
- Williams, T. (2008). Animal models of ventral body wall closure defects: a personal perspective on gastroschisis. *Am J Med Genet C Semin Med Genet* 148C, 186-191.
- Wojcik, S. M., Katsurabayashi, S., Guillemin, I., Friauf, E., Rosenmund, C., Brose, N., and Rhee, J. S. (2006). A shared vesicular carrier allows synaptic corelease of GABA and glycine. *Neuron* 50, 575-587.
- Wu, W. L., Ziskind-Conhaim, L., and Sweet, M. A. (1992). Early development of glycine- and GABA-mediated synapses in rat spinal cord. *J Neurosci* 12, 3935-3945.
- Wu, Y., Buzzi, A., Frantseva, M., Velazquez, J. P., Cortez, M., Liu, C., Shen, L., Gibson, K. M., and Snead, O. C., 3rd (2006). Status epilepticus in mice deficient for succinate semialdehyde dehydrogenase: GABAA receptor-mediated mechanisms. *Ann Neurol* 59, 42-52.
- Wu, Y., Wang, W., Díez-Sampedro, A., and Richerson, G. B. (2007). Nonvesicular inhibitory neurotransmission via reversal of the GABA transporter GAT-1. *Neuron* 56, 851-865.
- Xie, H., and Ziskind-Conhaim, L. (1995). Blocking Ca(2+)-dependent synaptic release delays motoneuron differentiation in the rat spinal cord. *J Neurosci* 15, 5900-5911.
- Yamada, J., Furukawa, T., Ueno, S., Yamamoto, S., and Fukuda, A. (2007). Molecular basis for the GABAA receptor-mediated tonic inhibition in rat somatosensory cortex. *Cereb Cortex* 17, 1782-1787.
- Yanagawa, Y., Kobayashi, T., Ohnishi, M., Kobayashi, T., Tamura, S., Tsuzuki, T., Sanbo, M., Yagi, T., Tashiro, F., and Miyazaki, J. (1999). Enrichment and efficient screening of ES cells containing a targeted mutation: the use of DT-A gene with the polyadenylation signal as a negative selection maker. *Transgenic Res* 8, 215-221.
- Zhou, L., Chillag, K. L., and Nigro, M. A. (2002). Hyperekplexia: a treatable neurogenetic disease. *Brain Dev* 24, 669-674.
- Zimmerman, E. F. (1985). Role of neurotransmitters in palate development and teratologic implications. *Prog Clin Biol Res* 171, 283-294.